FEBRUARY 2022

IN COMPLIANCE™

THE COMPLIANCE INFORMATION RESOURCE FOR ELECTRICAL ENGINEERS

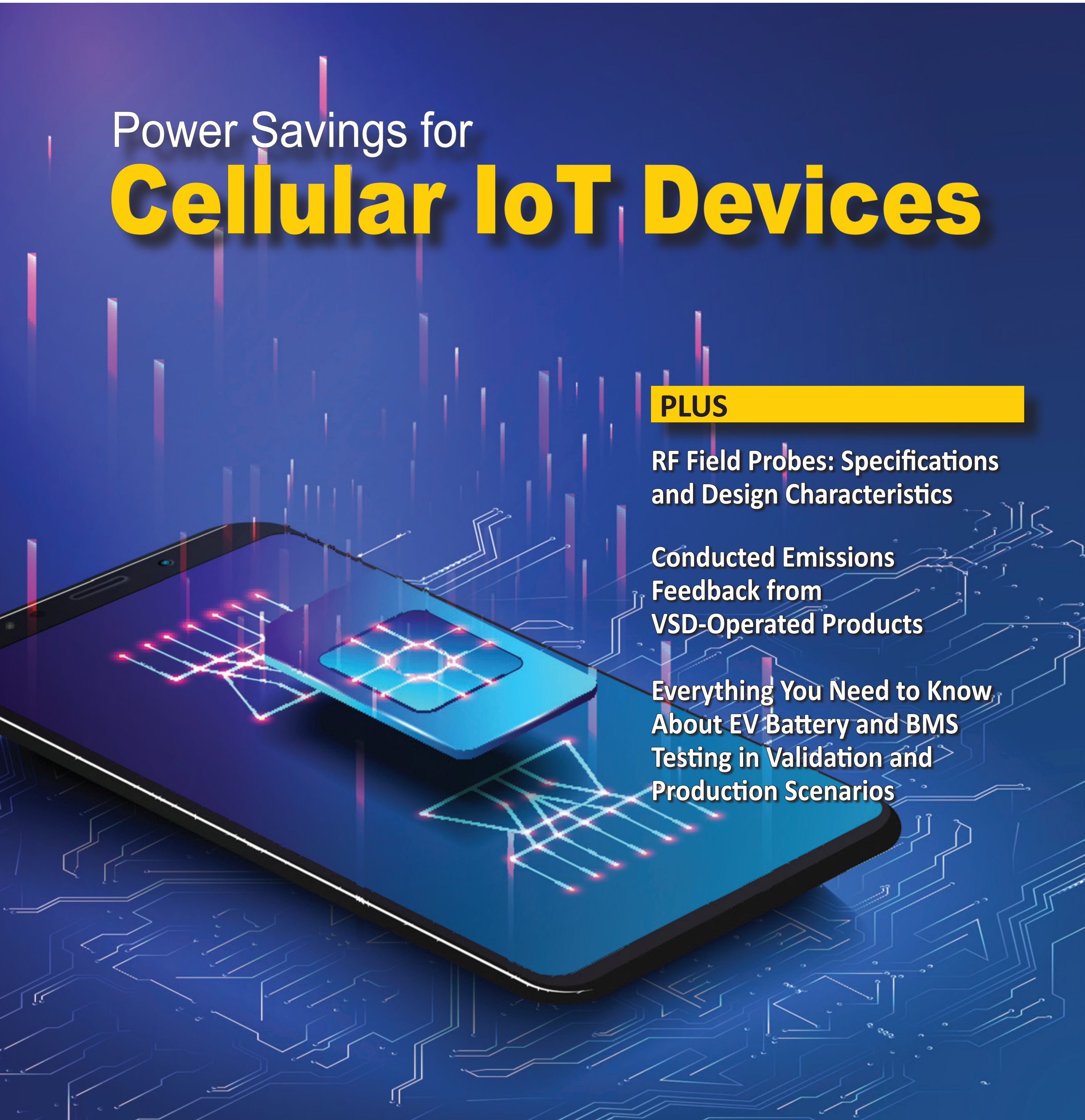

Power Savings for Cellular IoT Devices

PLUS

RF Field Probes: Specifications and Design Characteristics

Conducted Emissions Feedback from VSD-Operated Products

Everything You Need to Know About EV Battery and BMS Testing in Validation and Production Scenarios

Exodus AMP2030D-LC
1.0–6.0GHz,
600W, 400W P1

Exodus AMP2030D-LC, ideal for broadband EMI-Lab, Comm. and EW applications. Class A/AB linear design for all modulations & industry standards. Covers 1.0-6.0GHz, producing 600W Minimum, 400W P1dB and 58dB minimum gain. Excellent flatness, optional monitoring parameters for Forward/Reflected power, VSWR, voltage, current & temperature sensing for superb reliability and ruggedness. Integrated in our compact 10U chassis weighing approx. 50kg.

Exodus 6.0-12.0GHz, 100W,
Broadband Amplifier

Exodus Broadband Amplifier model AMP3085A covers 6.0–12.0GHz and produces >100 Watts minimum power 120W nominal. The AMP3085A has a minimum gain of 50dB with -25dBc harmonics. The unit is a compact Linear Class A/AB design for optimum reliability & ruggedness for all applications. Including current, temperature sensing and shutdown functions. Nominal dimensions of 180W x 200L x 27H mm with SMA-Female Input & N-Female RF Output connectors.

Exodus AMP2065A-LC,
6.0–18.0GHz, 200 Watts,
another outstanding TWT replacement

Exodus AMP2065A-LC is designed for replacing aging TWT technology.
A broadband, rugged EMC Class A/AB linear design for all modulations & industry standards. Covers 6.0-18.0GHz, produces >200W with a minimum 53dB gain. Excellent flatness, optional monitoring parameters for Forward/Reflected power, VSWR, voltage, current & temperature sensing for superb-reliability. Exodus Quiet-Cool technology in our compact 7U-chassis.

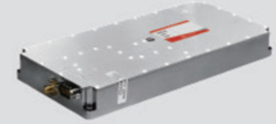

Exodus AMP1146A,
2.0 – 8.0GHz, 70W,
Solid-State Module replaces aging TWT's

Exodus Advanced Communications introduces our compact 2.0-8.0GHz Module. This ideal TWT replacement produces 70-watts minimum, 80-90W nominal power. The minimum power gain is 48dB with <-20dBc harmonics. Included are current & temperature sensing and built-in protection circuits for optimum reliability & ruggedness for all applications. The nominal weight is 3lbs, and dimensions of 4.3"W x 7.8"L x 1.0"H.

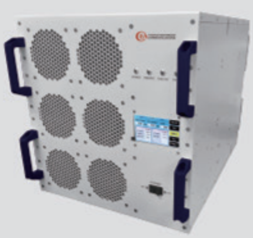

4KW S-Band (2.0–4.0GHz)
Solid State Pulse Amplifier–

Exodus Advanced Communications' Pulse Amp (2.0-4.0GHz, 4KW Pulse) is designed for Pulse/HIRF, EMC/EMI Mil-Std 461/464 and Radar applications. Other frequency ranges & power levels available all providing Superb Pulse Fidelity. Up to 100usec pulse widths, up to 6% duty cycles with a minimum 66dB gain. Available monitoring parameters for Forward/Reflected power in Watts & dBm, VSWR, voltage, current, temperature sensing for outstanding reliability and ruggedness in a compact 10U chassis.

Exodus AMP1158A,
700MHz – 6.0GHz, 30W,
Ultra-Compact Module

Exodus Advanced Communications introduces our Ultra-Compact 700MHz-6.0GHz lightweight Module. This module produces 25-watts minimum, 30W nominal power. The minimum power gain is 44dB with <-20dBc harmonics. Included are current & temperature sensing and built-in protection circuits for optimum reliability & ruggedness for all applications. The nominal weight is 450 grams, and dimensions of 75W x 105L x 30H mm.

EXODUS Engineering
Always Innovating

High Power Solid State Power Amplifiers

Modules & Systems

Broadband, CW, Pulse & Linear Applications

10kHz to 51GHz, 3KW CW, 50KW Pulse

Chip & Wire Hybrid Assemblies

Class A/AB Designs

Medium Power Amplifiers

10khz to 51GHz, 2W P1dB and below

Low Noise Amplifiers

New! Synthesizers

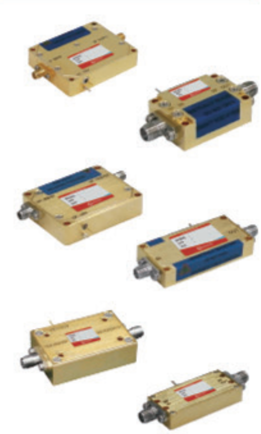

3674 E. Sunset Road, Suite 100
Las Vegas, Nevada 89120 USA
Tel : 1-702-534-6564
Email : sales@exoduscomm.com

www.exoduscomm.com

In Compliance Magazine
ISSN 1948-8254 (print)
ISSN 1948-8262 (online)
is published by

Same Page Publishing Inc.
451 King Street, #458
Littleton, MA 01460
tel: (978) 486-4684
fax: (978) 486-4691

IN COMPLIANCE

FEBRUARY 2022 CONTENTS

Volume 14 | Number 2

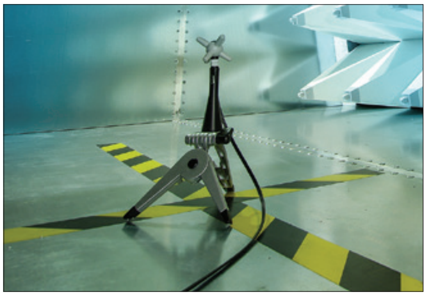

EU Commission Updates Harmonized Standards for Various Electrical Devices

The Commission of the European Union (EU) has updated its list of harmonized standards that can be used to demonstrate conformity with the safety requirements of the EU's Radio Equipment Directive (2014/35/EU, or RED).

Commission Implementing Decision (EU) 2021/2273 specifically updates harmonized standards originally detailed in Annex I and Annex II of Commission Implementing Decision (EU) 2019/1956. Compliance with the requirements of applicable harmonized standards in (EU) 2019/1956 confers a presumption of conformity with RED requirements.

New harmonized standards addressed in the update cover a variety of electrical and electronic products, including laser products, adjustable speed electrical power drive systems, power electronic converter systems and equipment, luminaires, low-voltage switchgear and control gear, uninterruptable power systems (UPS), and certain other electrical equipment designed for use within certain voltage limits.

Popular WiFi Routers Open to Cybersecurity Vulnerabilities

A number of popular models of WiFi routers contain software defects and other vulnerabilities that make them susceptible to cybersecurity breaches.

Those are the findings of a recent study by researchers at the IoT Inspector platform and German IT magazine CHIP, who found a total of 226 potential WiFi security vulnerabilities in routers manufactured by nine companies, including Asus, D-Link, Netgear, and Linksys. Individual routers with the largest number of identified individual vulnerabilities were the TP-Link Archer AX6000 with 32 vulnerabilities and the Synology RT-2600ac router with 30 vulnerabilities.

A summary of the results of the study was published in early December in an article on the TechTimes website. The TechTimes article also notes that the single biggest action that users can take to protect their routers from cyberattacks is to change the router's settings to allow automatic updates.

EU Commission Regulates Electronic Instructions for Medical Device Use

The Commission of the European Union (EU) has also published requirements for providing medical device instructions in electronic form under the scope of the EU's Medical Device Regulation (EU 2017/745, or the MDD).

Commission Implementing Regulation (EU) 2021/2226 represents a detailed, article-by-article supplement to the MDD on the conditions under which instructions for the use of medical devices may be provided in electronic form. The Regulation will help expand the use of non-paper-based instructions that can contribute to reduced environmental impact while also lowering manufacturers' costs.

At the same time, however, the Regulation clearly notes that providing instructions on the use of medical devices in electronic form "should be limited to certain medical devices and accessories intended to be used under specific conditions," and that "for reasons of safety and efficiency, users should always have the possibility to obtain those instructions for use in paper form upon request."

FDA Publishes Discussion Paper on 3D Printing of Medical Devices

The U.S. Food and Drug Administration (FDA) has released a discussion paper on the use of so-called 3D printing technology in the production of medical devices in hospitals and doctors' offices.

The paper, "3D Printing Medical Devices at the Point of Care (PoC)," provides extensive background on the FDA's current regulation of devices and 3D printing technologies, as well as key challenges to device safety and effectiveness presented by the use of such technologies. The paper also poses 16 different questions on the 3D printing of medical devices to garner input from the medical device industry, healthcare facilities and providers, and other stakeholders.

The FDA says that stakeholder input will "help build the foundation for an appropriate regulatory approach for 3D printing at the point of care, personalized care for patients and new innovations in this area."

FCC Settles Over Violation of Equipment Marketing Rules

The Enforcement Bureau of the U.S. Federal Communications Commission (FCC) has reached a settlement with an aviation electronics company over the illegal marketing of products.

According to an Order, the company, uAvionix, marketed some of its aviation devices to government contractors in the U.S. prior to receiving FCC equipment authorization for those devices. FCC rules require manufacturers of radio transmitters and other electronic devices that emit radiofrequency radiation to obtain the requisite authorization prior to marketing those devices to minimize the risk of interference with authorized communications.

As part of the settlement, uAvionix has admitted that it violated the Commission's rules and will pay a $13,000 civil penalty. The company has also agreed to implement a compliance plan to prevent future such rule violations.

FCC Reaches Major Settlements Over 911 Communications Failures

The Enforcement Bureau of the U.S. Federal Communications has entered into Consent Decrees with four major telecom carriers in connection with a system outage that prevented them from delivering 911 emergency calls.

The companies, CenturyLink, Intrado Safety Communications, Cellco Partnership (d/b/a Verizon Wireless), and AT&T Mobility, have agreed to pay a total of nearly $6.3 million in financial penalties for their roles in four separate 911 outages in September 2020. The outages ranged in length from one to three hours and affected users in multiple states across the U.S.

Commission rules require that "all telecommunications carriers shall transmit all 911 calls to a PSAP (public safety answering point), to a designated statewide default answering point, or to an appropriate local emergency authority." Carriers are also required to notify designated parties at the affected PSAP "as soon as possible but no later than thirty minutes after discovering the outage."

In addition to paying the designated financial penalties, each company also agreed to implement a compliance plan to ensure future compliance with FCC rules and to appoint a compliance officer to monitor the plan's implementation and effectiveness.

FCC Issues Annual Report on Robocalls

The U.S. Federal Communications Commission (FCC) has released its annual report to Congress, detailing consumer complaints and enforcement action in connection with illegal robocalls.

The report offers insight into trends related to informal consumer complaints regarding robocalls that were received by the Commission over five full calendar years, from 2016-2020, as well as complaint data and information about enforcement actions through November 2021.

Informal consumer complaints increased dramatically during the first three years covered by the report, from just under 180,000 in 2016 to more than 330,000 in 2018. Total consumer complaints then dropped significantly in the following two-year period, with 271,000 complaints filed in 2019 and just over 212,000 in 2020. However, the first 11 months of 2021 indicate a slight increase over 2020 levels, with more than 214,000 complaints submitted during the period.

The FCC's Enforcement Bureau has significantly stepped-up actions against robocall operators in recent years. The Commission issued two Notices of Apparent Liability for Forfeiture during 2020, with proposed forfeitures totaling nearly $250 million. The proposed forfeiture amounts included a record $225 million fine against two men reportedly responsible for making approximately one billion spoofed robocalls during the first half of 2019. During the first 11 months of 2021, the Commission issued only one Notice of Apparent Liability for Forfeiture, proposing a $5 million fine.

Walmart Accused of Dumping Hazardous Waste

The Office of the California Attorney General has filed suit against retail giant Walmart for allegedly dumping more than one million batteries, electronic waste, and other products with hazardous environmental effects into California landfills each year.

According to a report posted to the website of CBS News, the suit was filed in December by the Attorney General's Office in conjunction with district attorneys in 12 California counties and the California Department of Toxic Substances. It alleges that Walmart illegally disposes of nearly 80 tons of hazardous waste each year, an estimate reportedly based on 58 separate inspections conducted by the state of trash compactors at Walmart stores throughout California between 2015 and 2021.

A spokesperson for the company contends that the lawsuit represents an effort by the Attorney General's office to force the retailer into a new settlement in connection with a 2010 investigation involving similar charges.

POWER SAVINGS FOR CELLULAR IoT DEVICES

A Look at the Essential Measures Recommended by 3GPP

Yong Shi received an M.Sc. in communications engineering from the Technical University of Munich. He joined Rohde & Schwarz in 2013 and focuses on the application development for the wireless market segment. His technical expertise is in the area of cellular wireless communications (5G, LTE etc.) and connectivity standards (Bluetooth, WLAN and UWB). Shi can be reached at yong.shi@rohde-schwarz.com.

By Yong Shi

In the past decades, the Internet has been booming and connecting people around the world. Current technology trends tell us that not only the people but also machine-type devices, e.g., household appliances, street facilities such as traffic lights, and connected vehicles, are going to be connected and communicate with each other. The Internet of Things (IoT) is a buzzword crossing all vertical industries. We are now, so to speak, in the dawn of the IoT era. With IoT technology, the world is getting increasingly smart. New concepts such as smart cities, smart homes, and smart agriculture are becoming a part of daily life and gradually changing our lifestyles.

Cellular IoT (CIoT) is considered one of the most attractive contributions to the IoT industry. The technologies referred to as licensed spectrum-based low-power wide-area (LPWA) access technologies are deployed in the GSM, LTE, or 5G new radio (NR) network and provide benefits with respect to quality of service, reliability, latency, and coverage range. Yet they also have the characteristics of low complexity, low cost, and low power consumption. CIoT technology provides the opportunity for enterprises to increase efficiency and improve value for the customer.

Standardized by the 3rd Generation Partnership Project (3GPP), CIoT is the general term for radio technologies known as LTE-M (for long-term evolution for machines) and NB-IoT (for narrow band-internet of things). As shown in Figure 2, the first machine type communication (MTC) standard based on LTE network (also called LTE-M) was specified in 3GPP Release 12. Starting with Release 13, 3GPP included NB-IoT technology under the scope of the standard. By the first NR Release 15, CIoT was already an integral part of the whole NR standardization effort.

Two future focuses for the 3GPP include ensuring a smooth integration from LTE-based CIoT to 5G core network and developing NR-based CIoT to serve IIOT applications where mobile broadband (MBB) communication and ultra-reliable low latency

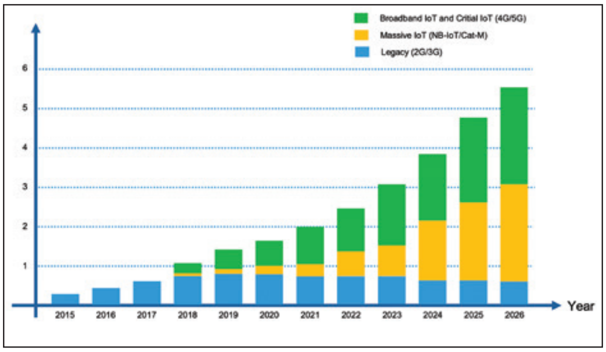

Figure 1: Cellular IoT connections by segment and technology (billion) (source: Ericsson Mobility Report, June 2021)

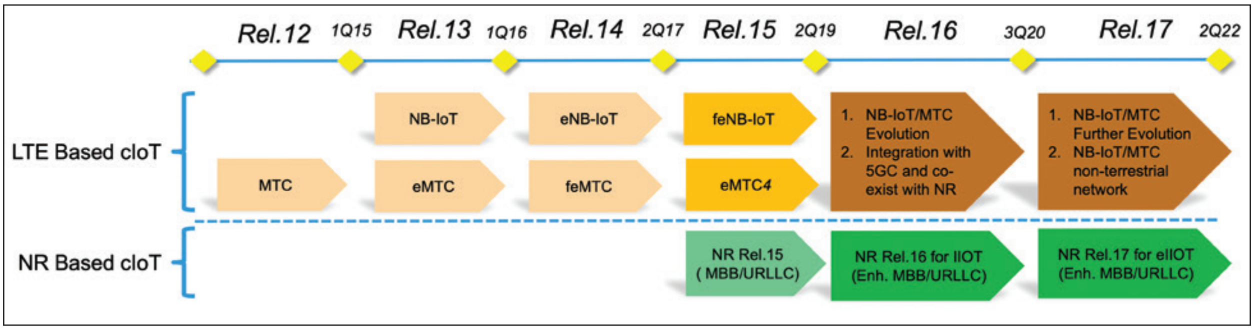

Figure 2: 3GPP cellular IoT (CIoT) evolution path

communication (URLLC) are required. The feature sets of both CIoT technologies are enhanced steadily along the entire evolution path, and power saving has always been a perpetual topic of the standard. In this article, we will shed light on some of the major power-saving measures for LTE-based CIoT implementations that are recommended by 3GPP.

POWER SAVING MECHANISMS

Discontinuous Reception (DRX)

Discontinuous reception (DRX) is a generic mechanism in mobile communication where the user equipment (UE) is allowed to stop monitoring the radio channel, e.g., physical downlink control channel (PDCCH), and enters the low power consumption mode or sleep mode for a certain period of time.

There are two types of DRX deployments, namely, idle DRX (i-DRX) and connected DRX (c-DRX) that correspond to the UE's radio resource control (RRC) idle and connected mode, respectively.

The UE operated in i-DRX mode monitors the PDCCH at defined time intervals. The UE will enter sleep mode between two consecutive PDCCH monitoring (see Figure 3).

In the c-DRX mode, the UE is allowed to monitor the PDCCH discontinuously to check if the scheduling messages can be detected by its cell radio network temporary identifier (C-RNTI) on PDCCH. Figure 4 illustrates the concept of a c-DRX process. Short DRX and long DRX cycles can be included in the c-DRX mode. The UE monitors the PDCCH during the On time and sleeps during the Off time in each DRX cycle. The DRX cycle starts when the DRX inactivity timer expires. The UE enters into a short DRX cycle(s) first, followed by a long DRX cycle. The adoption of a short DRX cycle is optional for LTE-M UE. However, NB-IoT UEs support only a long DRX cycle.

Extended Discontinuous Reception (eDRX)

Extended discontinuous reception (eDRX) is a power-saving optimization feature introduced in 3GPP Release 13. As the name implies, eDRX supports a longer DRX or paging cycle compared to the legacy DRX power-saving features described in the previous section.

Figure 5 shows the basics of eDRX in comparison to the legacy DRX where the DRX cycle is extended from 2.56 seconds to minutes or even hours. In an RRC idle state, a UE can be configured for up to approximately 44 minutes for LTE-M and approximately 3 hours for NB-IoT.

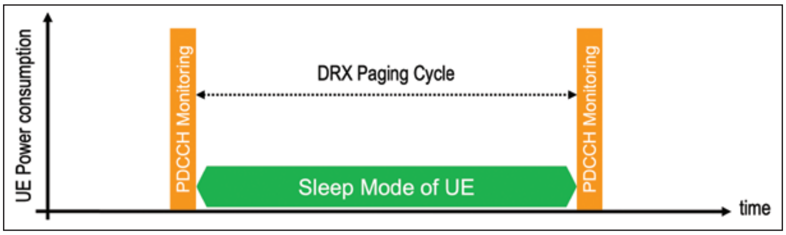

Figure 3: DRX in RRC idle mode (i-DRX)

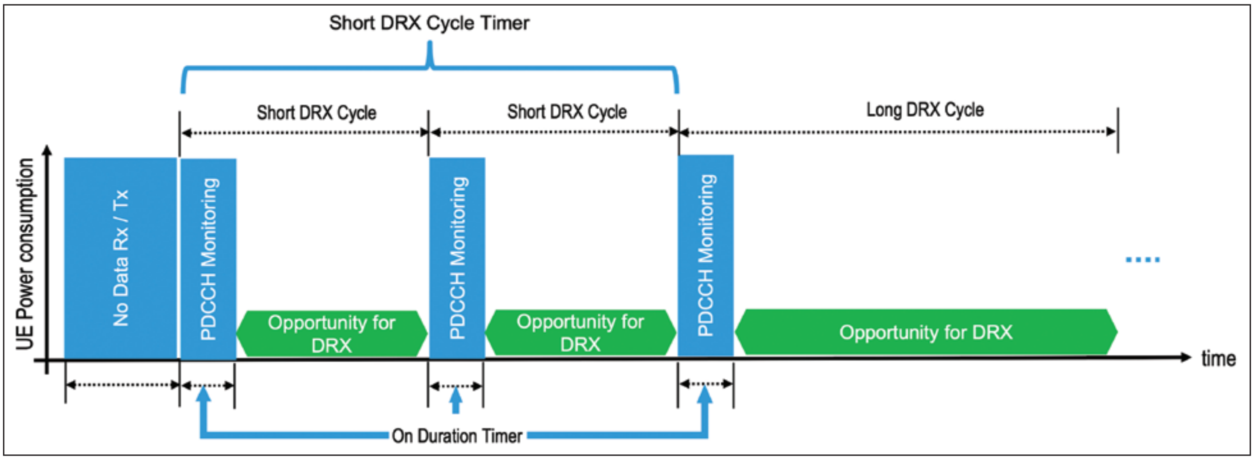

Figure 4: DRX in RRC connected mode (c-DRX)

Of course, the extension of DRX or paging cycle has the side effect where the UE becomes less responsive, i.e., mobile terminated connections will show a much longer call setup behavior. However, for some particular CIoT use cases, this drawback is acceptable. Typically, those CIoT UEs send a small amount of data and the data that has been sent or received is not time-critical, leading to more delay tolerance. Furthermore, there is an assumption that LTE-M and NB-IoT UEs have more uplink-oriented data traffic than the downlink ones. Therefore, the tradeoff between UE reachability and power consumption in these CIoT applications is now more in favor of reducing energy consumption. Long battery lifetime, for example, a minimum of 10 years, is required for LTE-M and NB-IoT UEs. To achieve this, an eDRX approach is highly recommended.

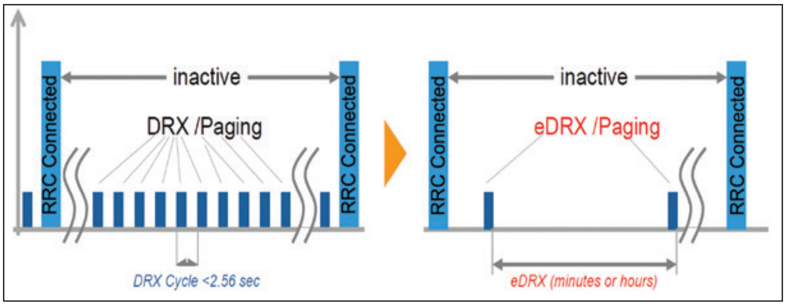

Figure 5: Comparison of DRX and eDRX

Power Saving Mode (PSM)

Power saving mode (PSM) is a feature designed for LTE-M/NB-IoT UEs to help conserve more battery power with its deep sleep characteristic. This feature was first introduced in 3GPP Release 12.

To update the network about its availability, the UE performs periodic tracking area updates (TAU) after a configurable TAU timer (T3412 timer) has expired. After that, the UE stays reachable for paging in the idle state for a period of time (T3324 timer). Once the T3324 expires, the UE enters the deep sleep mode, also called power-saving mode (PSM), becomes dormant, and is therefore unreachable until the next periodic TAU occurs.

During the PSM, the UE turns off its circuitry but is still registered in the network, meaning that the UE still keeps the non-access stratum (NAS) status while closing the access stratum (AS) connection. The advantage of such an approach is that the UE can wake up immediately from the PSM without having to reattach or re-establish the packet data network (PDN) connections. This avoids extra power consumption due to the transmission of additional signaling messages required for establishing a higher layer connection.

Figure 6 on page 14 indicates the principle of the PSM and its message flow. The UE can exit PSM either after the expiration of the T3412 timer, i.e., renewed TAU, or when the UE initiates a mobile originated

(MO) service or detach. With the latter, the UE can proactively exit PSM and enter the RRC idle state and connected state later to ask for the service.

The utilization of PSM is particularly interesting for use cases requiring infrequent mobile-terminated or mobile-originated events which allows the certain latency of the services, for example, a water meter sends the counter once a month. With a PSM mechanism, a 10-year battery lifetime, as recommended for the LTE-M and NB-IoT UEs, becomes possible.

Release Assistance Indication (RAI)

Release assistance indication (RAI) for access stratum (AS), a 3GPP Release 14 feature, allows the LTE-M/NB-IoT UE to trigger a buffer status report (BSR) with zero-byte size to indicate to the eNB that it has no more uplink data, and that the UE does not anticipate receiving further downlink data. This makes it possible for the RRC connection to be released. As a result, the early transition from the RRC connected state to RRC idle state to save power is enabled. Without having the RAI introduced, the UE would have to wait for the eNB to release the connection via explicit signaling or when the RRC inactivity timer expires.

Mobile Originated Early Data Transmission (MO-EDT)

In 3GPP Release 15, CIoT data transfer in the control plane (CP) and the user plane (UP) modes is enhanced to the so-called CP-EDT and UP-EDT, respectively. In contrast to the legacy data transfer using CP and UP CIoT EPS optimization defined in Release 13, the main benefit of the EDT lies in the fact that

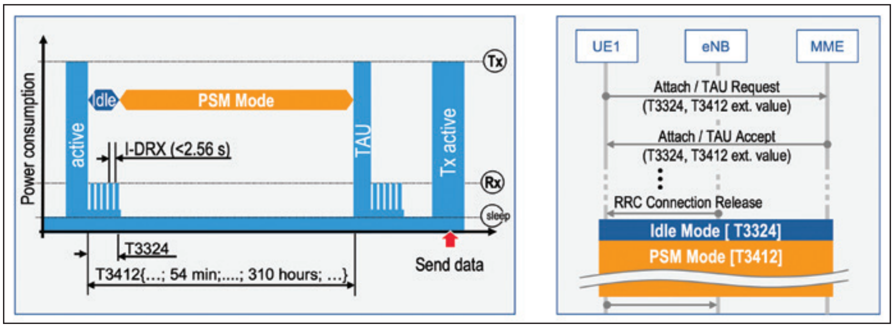

Figure 6: Principle of power-saving mode

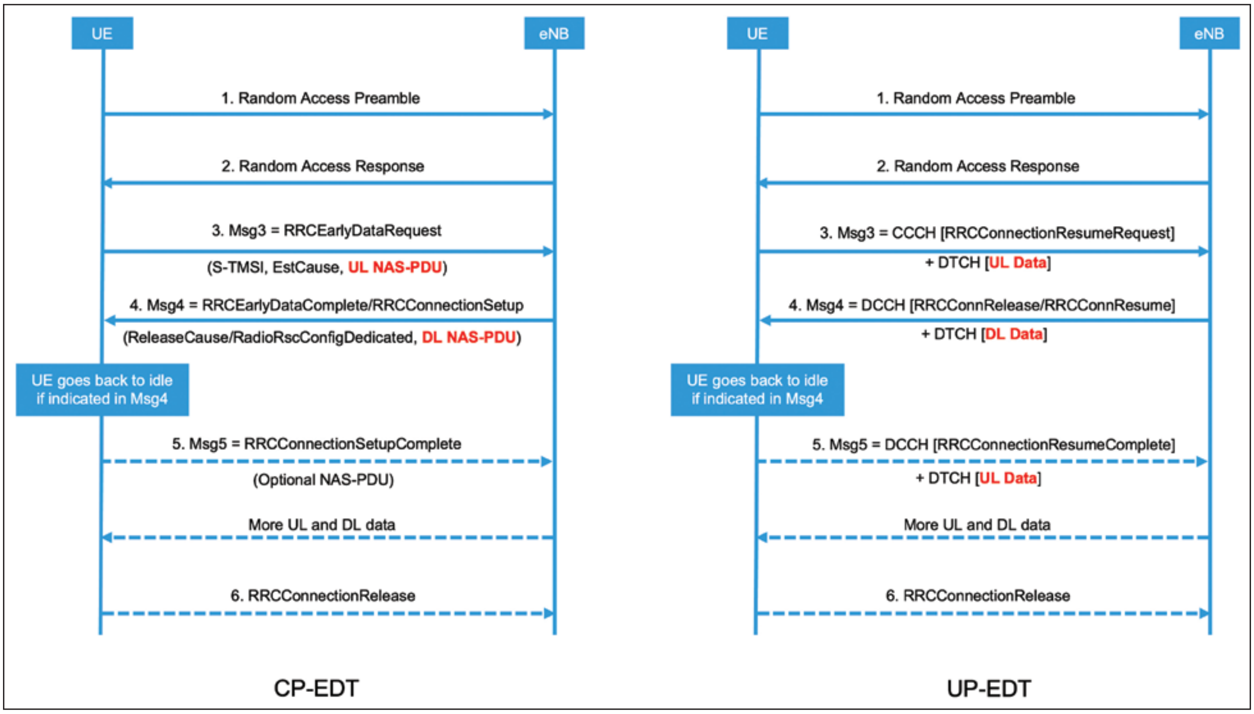

Figure 7: Signaling flow of mobile-originated CP-EDT and UP-EDT including data transmission fallback

the uplink and downlink data can be transmitted early during the contention-based random access (CBRA) procedure.

Uplink and downlink data can already be sent together with message 3 (Msg3) and message 4 (Msg4), either piggybacked (CP-EDT) or multiplexed (UP-EDT) with the RRC message. The procedure could actually terminate after Msg4 if no more data has to be received or transmitted by the UE. The approach reduces the signaling overhead as well as message latency and therefore lowers the UE's power consumption. Specifically, battery life can be improved by almost three years and the message latency is reduced by more than three seconds under poor radio conditions compared to performance under Release 13.

Certain maximum transport block size (TBS) is expected by EDT. For an LTE-M UE, TBS given in Msg3 is dependent on the coverage enhancement (CE) level. For CE0 and CE1, the UE can utilize the maximum 1000 bits TBS to transmit data, whereas for CE2 and CE3, the UE is only allowed to apply maximum 456 bits TBS. For an NB-IoT UE, the maximum TBS is about 1000 bits.

RRC message in Msg4 implicitly communicates whether more data has to be exchanged. By receiving the message "RRCEarlyDataComplete/RRCConnectionRelease," the UE understands that the eNB has no more data to transmit and can go to RRC idle mode. Otherwise, by receiving the message "RRCConnectionSetup/RRCConnectionResume," the UE will expect more data from eNB and fall back to legacy mode (Release 13) by establishing/resuming the connection.

Figure 7 shows the signaling flow of the CP-EDT and UP-EDT. The message flow plotted in the dotted line indicates the Release 13 CIoT UP and CP which serves the fallback procedure of the data transmission. This happens when more UE data is expected to be sent.

Mobile Terminated Early Data Transmission (MT-EDT) [5]

3GPP Release 16 extends the EDT feature to mobile-terminated EDT (MT-EDT) as well, intended for a single downlink data transmission. It allows the downlink data transmission during the random access (RA) procedure triggered in response to a paging message. Depending on the received data size from the core network, eNB can decide whether MT-EDT should be initiated or not. If MT-EDT occurs, the UE is informed by the MT-EDT indication added by eNB in the paging message. Subsequently, the UE triggers the EDT procedure which can be based on CP-EDT or UP-EDT, as presented in Figure 8. The difference to MO-EDT is that it does not contain the UL data in Msg3 of the RA procedure here.

Preconfigured Uplink Resources (PUR)

Preconfigured uplink resources (PUR) represent an additional aspect of the power saving mechanism defined in 3GPP Release 16. As depicted in Figure 9, the UE requests PUR configuration (number of occurrences, periodicity, time offset, TBS, etc.) in RRC connected state towards eNB. The eNB then decides to provide the PUR resource to the UE and at the same time sends the UE to RRC idle state with the message "RRCConnectionRelease." By the subsequent uplink data transmission, instead of acquiring resources through the RA procedure, the UE transmits UL data by utilizing MO-EDT ("RRCEarlyDataRequest/RRCConnectionResumeRequest" in Msg3) on the

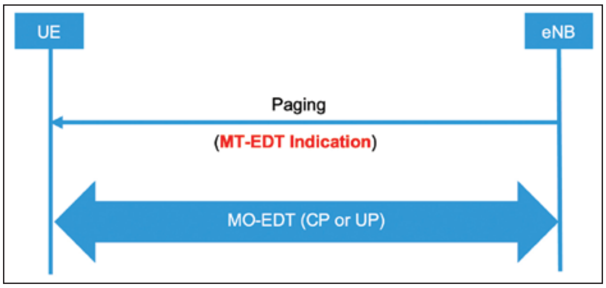

Figure 8: Signaling flow of mobile terminated EDT

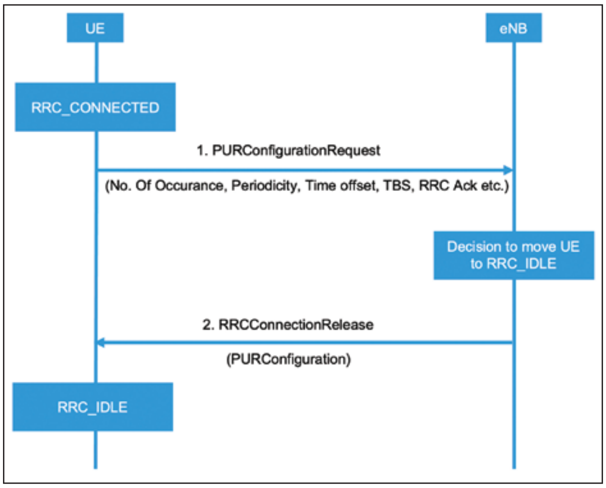

Figure 9: PUR configuration request

agreed PUR resource. In this case, Msg 1 and 2 of the RA procedure can be waived, and the uplink transmission power efficiency is increased.

Wake-Up Signal (WUS)

A wake-up signal (WUS) is a 3GPP Release 15 feature which is similar to the UMTS paging indicator channel. It is a physical signal in conjunction with DRX operation that can be decoded or detected before the UE monitors the paging on PDCCH. The benefit of introducing WUS is to reduce unnecessary power consumption related to the PDCCH monitoring. By having the WUS approach, the UE only needs to decode the PDCCH when WUS is detected; otherwise, the UE will stay in the sleep mode. This represents an efficiency improvement, especially when considering low activity periods on the control channels within a cell, e.g., at nighttime. Figure 10 illustrates the WUS principle in comparison to the conventional i-DRX operation.

The timing of the WUS with respect to the associated PO is shown in Figure 11. WUS duration is the maximum time duration that is configured by the network for the UE to detect the WUS. After the WUS is detected, the network leaves gap time to allow the UE to re-synchronize to the network and eventually switch over from the low-power wake-up receiver to main baseband circuitry in order to be ready to decode the PDCCH.

To ensure that the UE does not miss any paging message, the WUS adopts a robust Zadoff-Chu sequence of length 131 to keep the missing detection rate below 1%.

The latest development of WUS is addressed in 3GPP Release 16. A so-called UE-group WUS (GWUS) was introduced [5]. With this evolution, eNB instructs the UEs in the defined group to monitor the paging on PDCCH. The intention of this is to reduce the false alarm rate. In principle, several UEs may be mapped to the same PO. With the Release 15 WUS, some UEs may be unnecessarily awakened by the WUS when the intention of the eNB was actually to page the other UEs associated to the same PO.

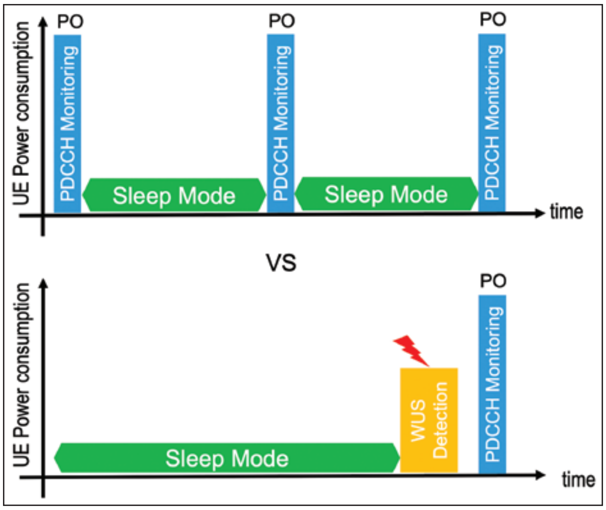

Figure 10: I-DRX vs. DRX with WUS detection

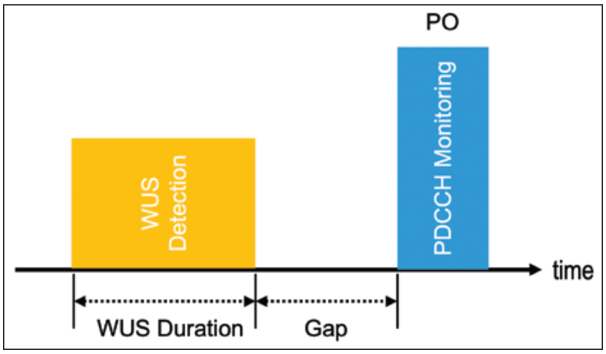

Figure 11: Timing of WUS

Power saving feature	3GPP Release
DRX	12[1]
Power saving mode (PSM)	12
eDRX	13
Release assistance indication (RAI)	14
Mobile originated early data transmission (MO-EDT)	15
Reduced system acquisition time	15
Relaxed monitoring for cell reselection	15
Wake-up signal (WUS) / UE-group wake-up signal (GWUS)	15/16
Mobile terminated early data transmission (MT-EDT)	16
Preconfigured uplink resource (PUR)	16
Increase peak data rate	17

Table 1: Summary of power-saving mechanisms in 3GPP releases for CIoT

[1] Legacy technology from GSM era. It was included in the very first MTC specification in 3GPP Release 12.

Reduce System Acquisition Time

Several features to reduce system acquisition time are specified in 3GPP Release 15. Their handling differs somewhat for LTE-M and NB-IoT UE. In the LTE-M case, several measures are included in the 3GPP Release 15 specification as explained in the following section.

After the UE is awake from a PSM or a DRX sleep mode, it usually needs to resynchronize with the network to acquire the time and frequency synchronization. This is typically due to the clock drift in the UE. In order to enable the UE to carry out fast time and frequency synchronization to save power, a newly designed resynchronization signal (RSS) is introduced. It is denser in time and frequency than the legacy PSS/SSS (still required for initial synchronization to a new cell). The potential power saving by using RSS can reach up to 98% in comparison to legacy PSS/SSS. Furthermore, RSS is also capable of indicating whether or not there are any changes in the MIB. Based on this, the UE may even skip decoding the MIB.

Furthermore, the UE may re-acquire SIB1 less often. This can be achieved by setting a flag bit in MIB indicating the change of SIB1 during the system information validity time. The UE shall read MIB after DRX or after cell reselection. If there is no indication of a change in SIB1, then the previous SIB1 stored in UE should be considered.

Improving the MIB and SIB demodulation performance is also addressed. The reduced acquisition time is enabled by enhanced cell global identity (CGI) reading delay requirements based on an accumulation of transmissions within two 40 ms periods for MIB and one modification period for SIB1/SIB2.

For NB-IoT UE operated in FDD mode, reduced system acquisition time is achieved during the cell access. This happens when eNB transmits SIB1-NB message (maximum 16 repetitions of SIB1-NB) in additional subframes on anchor carriers and non-anchor carriers. This approach enables the UE to decode the SIB1-NB faster, thus contributing to the power saving.

Relaxed Monitoring for Cell Reselection

This feature intends to reduce the radio resource management (RRM) monitoring during the cell reselection procedure when the NB-IoT UE has low mobility or is not at the cell edge. Network signals the UE with an NB-IoT reference signal received power (NRSRP) delta threshold. When the changes in RSRP in the current cell do not exceed the given threshold, then the UE does not need to monitor the neighbor cells for 24 hours. With this approach, the UE power consumption is reduced.

Increase the Peak Data Rate

Several feature proposals regarding 3GPP Release 17 standardization are currently being discussed. One of the main objectives is to increase the peak data rates for NB-IoT and LTE-M. This is intended to support the broadening use cases for cellular LPWA IoT, addressing the lessons drawn from deployment and trials, and supporting the long-term lifecycle of NB-IoT and LTE-M. This throughput increase will indirectly achieve power saving by allowing the UE to terminate the connection earlier, or by entering into a lower power mode sooner. For example, supporting 16-QAM for unicast in UL and DL for NB-IoT UE. For LTE-M UE, 14-HARQ processes in DL for half-duplex FDD mode, maximum DL TBS of 1736 bits for half-duplex FDD in CE Mode A.

CONCLUSION

CIoT (LTE-M and NB-IoT) technology is gaining more and more momentum and its evolution continues in the 5G era. At the same time, the massive scale of CIoT poses a big challenge to network efficiency, user experience, and field service efforts. Thus, introducing power-saving mechanisms for CIoT technology are essential.

In this article, we touched upon a few of the common power-saving measures specified by 3GPP. They cover the feature optimization on the physical layer right up to the RRC layer. Different aspects such as reducing downlink monitoring (enter sleep mode to save power), faster release of the RRC connection, minimizing signaling overhead, and enabling the fast system acquisition can contribute to the overall power saving of the CIoT UE.

The evolution of the power saving techniques is an ongoing process and further enhancements are foreseen in the future IoT application based on non-terrestrial networks. Stay tuned and be excited.

RF FIELD PROBES: SPECIFICATIONS AND DESIGN CHARACTERISTICS

Ensuring the Accuracy of RF Measurements in the Field

RF (radio frequency) field probes are an essential piece of equipment used for measuring the intensity of radiated RF fields. Although this instrument is crucial in implementing a radiation immunity test system, system specifiers often gloss over this essential element after spending a considerable amount of time and energy selecting amplifiers, antennas, and other equipment to generate the required RF field. A live test using a field probe will then determine if the RF test system's expected performance has been achieved.

These specialized RF measuring instruments carry a unique set of specifications. Understanding the specification definitions, field probe design characteristics, and other varying features will, in turn, allow a confident and informed decision in choosing a suitable field probe.

FIELD PROBES SPECIFICATIONS

Frequency Response or Frequency Range

The frequency response of a probe is one of the first probe specifications to consider and is the frequency range over which the probe's performance is defined. Since no probe can provide a completely flat response across the entire frequency range, this specification is accompanied by a tolerance figure, generally provided as a ±dB-allowable variation band.

An example of a frequency response curve is shown in Figure 1. If the probe does not cover the entire frequency range of the test application, multiple probes may be required.

Sensitivity

The sensitivity of a probe determines the lowest field level the probe can accurately measure and is important to consider when low field levels need to be

Pat Dayton is an Applications Engineer at AR RF/Microwave Instrumentation and can be reached at pdayton@arworld.us.

By Pat Dayton

measured. Some specifications call for a field level of 1 V/m or even less, which may be below the sensitivity of many probes, or very close to its noise floor. The most sensitive probes can accurately measure a few hundred mV/m.

Field Strength Range

Field strength range is the amplitude range of RF field levels a probe can read. The greater this range, the better a probe is suited for test applications that span a wide range of test levels. An example of field strength range is 0.5 - 800 V/m.

Dynamic Range

Dynamic range, used in the context of field probes, is closely related to the field strength range. Dynamic range conveys the magnitude between the lowest and highest specified field strengths (the field strength range), expressed in logarithmic units of decibels (dB). As an example, a field strength range of 0.5 - 800 V/m is expressed as 64 dB dynamic range.

Overload or Damage Level

This rating refers to the field level where damage can occur to the probe. Care should always be taken not to exceed this field strength with the probe present, even if the probe is turned off. Overload can be stated as a max pulsed level or a CW level, for example, 1000 V/m CW.

Isotropic Deviation

The variation of the probe's response from ideal as it is rotated in the field is called isotropic deviation. While this deviation in measurement is usually verified at one frequency and in one rotational plane, some advanced probe calibrations can offer a more extensive calibration with isotropic response measurements taken at multiple frequencies.

The graphic shown in Figure 2 on page 20 shows a typical isotropic response of a probe. If calibration factors were applied to each axis, the resultant curve would approach an ideal concentric circle or

Linearity

The linearity spec is a measurement of deviation from an ideal response over the probe's dynamic range. Linearity data is provided since an RF probe's response may vary somewhat as a function of the applied field level. This characteristic can cause some variation in accuracy when testing at levels other than that used during calibration. For example, one might encounter a variation of ±0.5 dB across a dynamic range of 0.5 – 800 V/m.

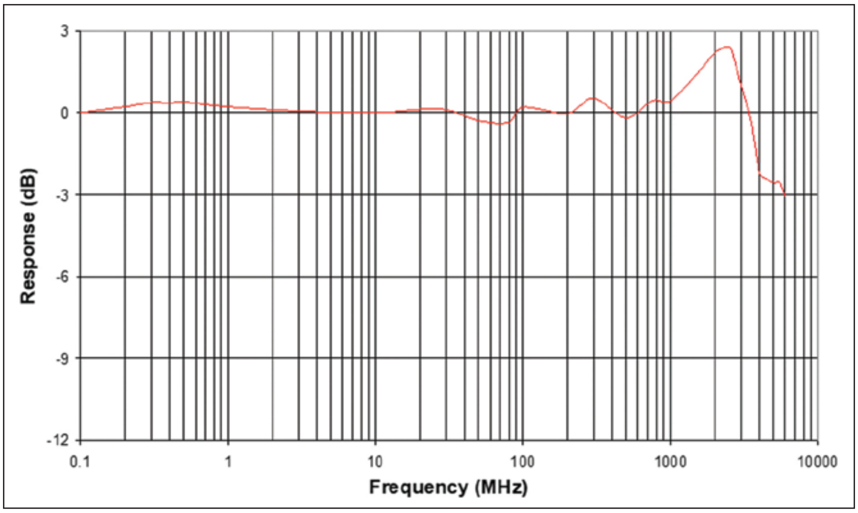

Figure 1: Frequency response curve example

completely isotropic. The term isotropic gives the impression that measurements are taken as the probe is rotated in every direction. However, this is not the case due to the time this would take, and the resultant calibration cost. An example of an isotropic deviation is ±0.5 dB, 0.5 MHz – 2 GHz.

Temperature Stability

The temperature stability is the deviation of the probe's reading over the operating frequency range as temperatures vary, for example, ±0.5 dB over the operating temperature range.

Control

Control refers to the method used to communicate with the probe. When performing EMC testing, fiber optic control is the only viable choice, as fiber optic cables are nonmetallic and will not interfere with the radiated immunity test setup. Furthermore, they are not susceptible to data corruption from voltage/current induced by the RF field.

FIELD PROBE DESIGN CHARACTERISTICS

E vs. H Fields

Probes are designed to either detect E (electric) fields or H (magnetic) fields. E-field probes are more commonly used in many EMC tests and cover a much larger frequency range than H-field probes. H-field probes are more commonly used at low frequencies, typically below 1 MHz.

CW vs. Modulated

The most common type of field probes are probes designed to measure non-modulated, continuous wave (CW) electric fields over a broad range of frequencies and amplitudes, and as such, these are commonly referred to as CW probes. This is the field probe type that has been used within the EMC industry for many years.

However, many EMC specifications use modulation in some form, primarily pulse modulation (PM) or amplitude modulation (AM). A CW-only field probe is not appropriate for measuring these signals, and an alternative type of probe needs to be selected based on the modulation being used.

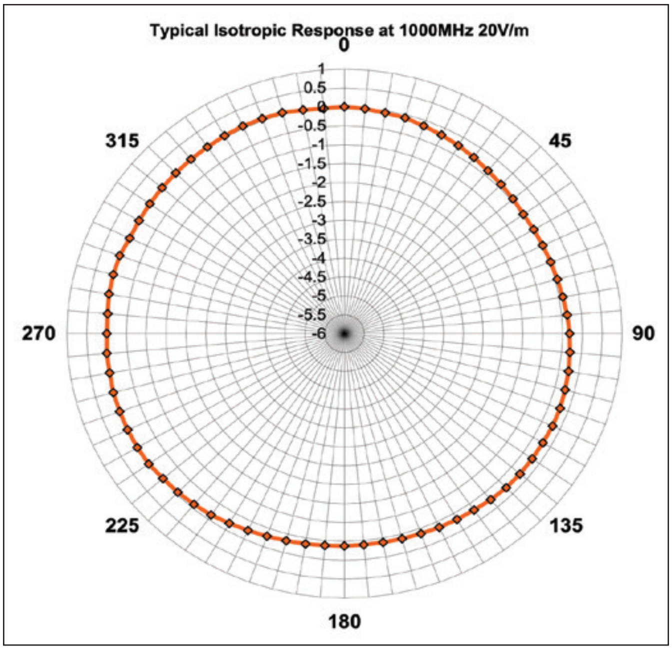

Figure 2: Typical isotropic response at 1000 MHz 20 V/m

The product specification sheet should be consulted to understand the probe's capability. Some probes are limited to specific modulation types, while others will measure CW, PM, and AM fields. When deciding on a field probe for measuring modulated fields, ensure that the probe selected is appropriate for the modulation being used. A CW-only field probe will often produce values in a modulated field. However,

EMC Standard	Modulation(s)
RTCA/DO-160	4% Duty 1 kHz Pulse
	90% Depth Square Wave 1kHz
	4uS Pulse 1 kHz Repetition Rate
IEC 61000-4-3	80% Depth 1 kHz AM
ISO 11452	3uS Pulse
	80% Depth 1 kHz AM Peak Conservation
MIL STD-461 (revisions E and later)	50% Duty 1 kHz Pulse
	50% Duty 400 Hz Pulse

Table 1: EMS standards and their associated modulation schemes

the readings will likely be erratic and would not be usable for field measurements. Consult the test standard being used for guidance on appropriate probe selection.

Table 1 provides some examples of test standards and associated modulation schemes.

Isotropic vs. Non-Isotropic

Most modern EMC field probes are isotropic, with the probe measuring the field level's total value and unaffected by field polarity. This total value is determined by combining the three different sensors' measurements. The sensors are mounted orthogonally (perpendicularly) to each other and are commonly referred to as X, Y, and Z. This configuration allows the detection of RF fields regardless of the probe orientation. Many current EMC standards require isotropic probes.

Some older probe designs, classified as non-isotropic, use a single sensor, and can only detect a single field polarity. With this type, the probe must be carefully oriented, with respect to the field, to perform field measurements. Most EMC test standards require isotropic probes, precluding the use of non-isotropic models in these cases. Consult the test standard being used for guidance on appropriate probe selection.

Composite-Only vs. Separable-Axis

Three-axis isotropic probes can be further differentiated as separable-axis or composite-only. Separable-axis probes allow detection and reporting of each axis's field intensity individually. In contrast, three-axis isotropic probes that only provide a single composite field value are categorized as composite-only probes. Some test standards require the use of separable-axis probes, while other standards do not have this requirement.

Stalk vs. Monopole-Over-Ground Plane

Field probes come in various physical configurations, with common configurations being stalk style and monopole-over-ground plane style.

The stalk style presents as an antenna ball on a pole, or stalk, remote from the probe's body, as shown in Figure 3.3. This configuration separates the RF sensors from the reflective electronic housing via a stalk, which provides performance benefits. Separating the sensor elements from the housing allows minimizing the size of the sensor elements (antennas) in the probe head, resulting in the ability to operate at higher frequencies while also reducing disturbance to the field being measured. Minimizing the housing/body size will also reduce the disruption of the field. While the stalk probe is an excellent approach, there may be limitations in usage due to the measurement location's physical constraints.

The monopole-over-ground plane style, seen in Figures 3.1 and 3.2, is typically seen as a metal cube or sphere, with three protruding orthogonal antenna elements. The cube or sphere body contains probe circuitry and acts as a ground plane for the antenna elements. The smaller overall physical size relative to the stalk probe may allow for use in applications where the stalk probe is too large.

Cube-style monopole-over-ground plane probes have a cubical-shaped body and come in various sizes. In general, the smaller the better since a small probe has less effect on the RF field resulting in improved performance.

Sphere-style monopole-over-ground plane probes are typically preferred over cube-style probes by housing the electronics in a sphere that inherently has less effect on the RF field. In addition, the minimal field distortion is not position-dependent since there are no flat probe surfaces to contend with, reducing measurement variation due to probe orientation. The result is that a spherical probe style yields a flatter frequency and isotropic response than a cube probe.

Diode Sensor vs. Thermocouple Sensor

Diode sensor probe type is currently the most common sensor used for RF field probes. Diodes have excellent sensitivity as well as a larger dynamic range than thermocouple sensors. However, diode sensors can have a non-linear response to modulated fields if steps are not taken in the probe's design to correct this effect.

An alternative sensor type is a thermocouple sensor. Thermocouple sensors can measure the average amplitude of a repetitive modulated field correctly; however, the modulation envelope would need to be known if a maximum reading was required.

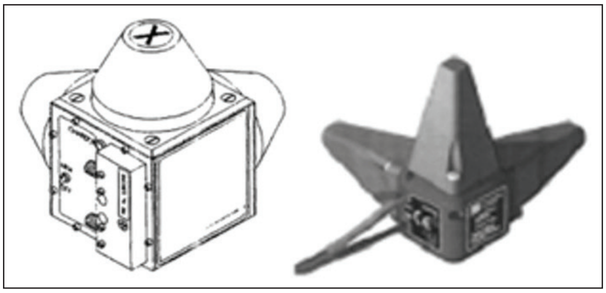

Figure 3.1: Cube-style monopole-over-ground plane probe

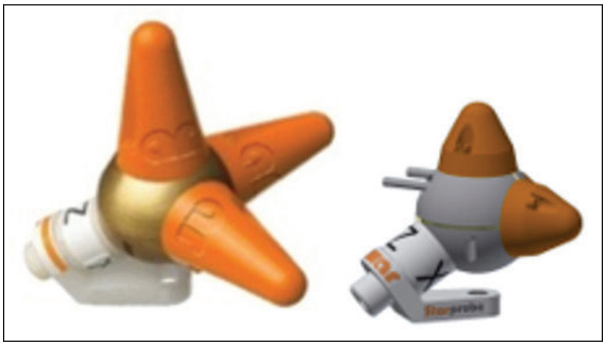

Figure 3.2: Sphere-style monopole-over-ground plane probe

Figure 3.3: Stalk-style probe

These sensors do not suffer from the same nonlinear response to modulated fields that diode type sensors do; however, thermocouple type sensors have a much slower response time than diode-based sensors. Since thermocouple probes are less sensitive and have a narrower dynamic range than diode-type probes, they are not commonly used in EMC immunity applications.

Laser vs. Battery Power

There are two methods of powering a field probe, battery power and laser power. Providing power to the probe using wires is not recommended since the metallic power cord would adversely affect field uniformity. Energy induced by the RF field in the power cord may introduce errors in the field measurements.

Battery-powered probes contain batteries in the probe housing. While battery-powered field probes and monitors are useful for hand-held mobile usage, the trade-off is reliability. Rechargeable batteries have a limited charge life as well as occasional failures. Since some probe vendors require that the probe be returned to the factory for battery replacement and recalibration, a simple battery failure can shut down an immunity test system. Running out of battery power in the middle of a test is also a limitation of battery-powered probes.

For applications that do not require the mobility provided by a battery-powered field probe, laser-powered probes have been designed to avoid the reliability issues encountered with rechargeable batteries. This power-over-fiber (PoF) system uses a high-energy laser driver to deliver laser energy to the probe via the same fiber optic cable used for communications. A converter within the probe converts the IR back to electricity to power the probe. Unlike a probe that relies on rechargeable batteries for power, a laser-powered probe can operate indefinitely, which translates to a vast improvement in reliability and productivity.

Laser safety must be considered whenever products are used that contain lasers. These products will fall into various categories dependent upon laser characteristics and power. Regardless, products containing lasers need to comply with safety standards that exist to protect the user. Product manufacturers must ensure their product design incorporates proper safety mechanisms and labeling to conform to the applicable safety standard requirements.

Temperature Compensation

If there were to be a significant variation of temperature between when the probe was calibrated and when the probe was used during a test, the probe reading would likely contain an error component due to this temperature variation. Some probe manufacturers supply a temperature correction equation that must be applied to correct for ambient temperatures that differ from the temperature at which the probe was calibrated.

Since high field levels and even operating EUTs can generate a great deal of heat, it is difficult to actually determine the dynamic heat fluctuation at any given moment, much less apply the correction factor. Thus, this cumbersome chore is often ignored, which introduces a source of error. Some manufacturers provide probe models with internal temperature compensation that automatically adjusts as probe temperature changes. For these probes, as long as the probe is used within its stated parameters, no additional temperature compensation is necessary, removing a source of thermal measurement error.

CONCLUSION

Field probes are specialized measuring devices and are available in various configurations and capabilities. Understanding these multiple configurations and functionality is critical when choosing a field probe. Frequency and dynamic range, E or H field, CW or modulated, composite or separable-axis, and laser or battery-powered are all important aspects to consider when selecting a probe. It is also important to review any test standards being used, as many test standards contain requirements for the field probe and thus should be consulted during the probe selection process.

Selecting the proper field probe with the appropriate characteristics and functionality is the first step toward performing RF field measurements. Once a probe is selected, using proper measuring techniques and best practices in operating the probe is important to achieve accurate measurements.

CONDUCTED EMISSIONS FEEDBACK FROM VSD-OPERATED PRODUCTS

What Can We Learn From Testing Actual VSD-Driven Products

Henry W. Benitez can be reached at henry@emicomply.com.
Aziz S. Inan can be reached at ainan@up.edu.
Christopher Miles can be reached at milesc18@alumni.up.edu.
Peter E. Perkins can be reached at p.perkins@ieee.org.
Joshua Thompson can be reached at joshua.thompson@intel.com.

By Henry W. Benitez, Aziz S. Inan, Christian Miles, Peter E. Perkins, PE, and Joshua Thompson

***Editor's Note:** The paper on which this article is based was originally presented at the 2020 IEEE International Symposium on Product Safety Engineering held virtually in November 2020. It is reprinted here with the gracious permission of the IEEE. Copyright 2021 IEEE.*

INTRODUCTION

Nuisance tripping of GFCIs (Ground Fault Circuit Interrupters) has given rise to questions about the role of conducted emissions from equipment using switching methods, such as VSDs (Variable Speed Drives), in causing a GFCI to trip. An earlier paper [1] described a test condition where several GFCIs would trip inadvertently under an applied Electrical Fast Transient (EFT) impulse; this false-positive result is normally considered nuisance tripping since the tripping cause was not determined. This follow-on paper provides additional data from testing aimed at looking at the line conducted emissions and ground lead touch current from some units while under actual operation using GFCIs.

Note that most GFCIs use the difference in line and return current to trigger protection; however, a common electric shock is from current in the earth/ground lead when this lead is not properly grounded. The differential line current is then a proxy for the earth/ground current hazard.

BACKGROUND

Although GFCIs could be tripped by test signals, having the actual signals being generated by the operating product would potentially provide specific threat information affecting GFCI operation that needs to be mitigated.

Some manufacturers were contacted and invited to supply residential or commercial units to be used for investigating these threats. Three such products were supplied for this evaluation.

For one of the products, the user had full control of the VSD in operating the unit. This product evaluated in this follow-on student GFCI research project had been involved in nuisance tripping complaints where the unit would not work when connected to one GFCI protected outlet but would work when connected to another outlet (each outlet separately GFCI protected, a common practice for electrical outlets provided on construction sites).

For the other two, the provided units operated from a programmed cycle which made the data collection more time-consuming and difficult as the VSD drive conditions changed throughout the duration time of the cycle.

This small collection of equipment tested provided substantial data which is summarized in this paper.

Safety in Electrical Systems

Electric shock is the physiological reaction or injury caused by electric current passing through the body. Figure 1 shows the effects of bipolar/AC current in terms of its magnitude and duration of time on the human body [2]. The summary provided in Figure 1 for each effect vary from person to person with the average values being highest for men, then women, then children [3]. The average startle-reaction level, 0.5 mArms/7.07 mApk, is the threshold value of current which can cause an involuntary reaction. The letgo-immobilization level, 5 mArms/7.07 mApk, is the maximum amount of current that can flow through a person who is experiencing electrical shock where he or she can still release and disconnect from the charged object. Currents above 5 mArms/7.07 mApk cause involuntary muscle contractions resulting in perspiration which lowers the body's resistance and increases current through the body [4].

Preventing currents from exceeding the letgo-immobilization threshold is important because more severe ventricular fibrillation can occur at currents as little as 30 mArms and cause death without medical intervention, especially CPR.

Variable Speed Drives (VSD) Basics

Variable-speed drive (VSD), describes an electronic controller used to control the speed of motors in equipment. Many products are expected to operate at different speeds depending upon their different usage. Where process or operational conditions demand adjustment of flow from a pump or a fan, varying the speed of the drive may also save energy compared with older techniques for control.

Variable speed drives can work with both AC and DC motors. Power electronics based VSDs are rapidly replacing older technologies for this purpose. VSDs provide smoother speed change for motors than older technologies as well as better operating efficiency. However, the electronic switching used also generates substantial harmonic impulses which conductively feedback into the line supplying power to the motor. The purpose of this work is to study this feedback.

TESTING PROCEDURE

Two sets of tests were run on each machine during operation; the touch current (earth/ground wire leakage current) test and the test of the conducted lines feedback flowing back into the power line feeding the unit. GFCIs were used during the testing confirming nuisance tripping conditions during normal operation.

During the touch current testing of the direct VSD driven unit, some of the GFCI units reported earlier [1] tripped in two instances during the operation under specific operating conditions. The determination of any particular part of the input signal which tripped the GFCI could not be determined. The programmed units, however, did not trip the GFCIs, although, unfortunately, it was determined after the testing that some conducted emission mitigation had already been implemented in these units. The EMC filters added are intended to reduce the high frequency components fed back on the line.

TIME/FREQUENCY DOMAIN ANALYSIS EXAMPLE

Working between the time and frequency domain is well understood analytically but not used much in practice traditionally by some electrical engineers.

Here is a simple analytical example to help bridge these two domains. This example is for a line

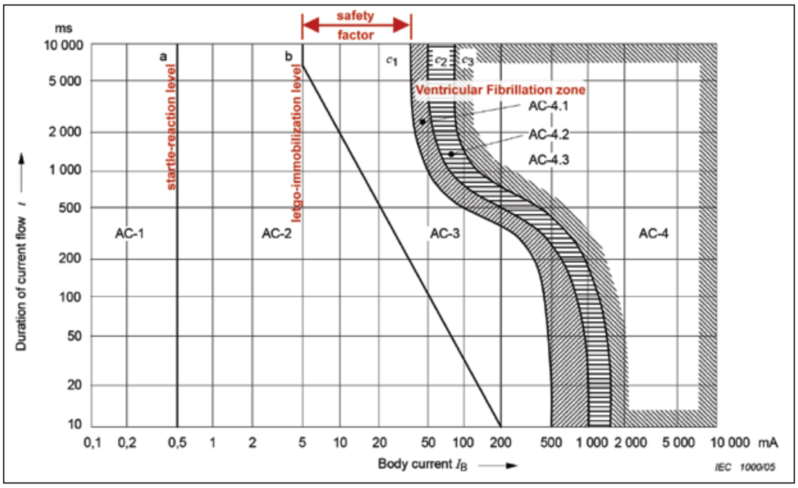

Figure 1: IEC 60479-1 AC current-time electric shock effects annotated

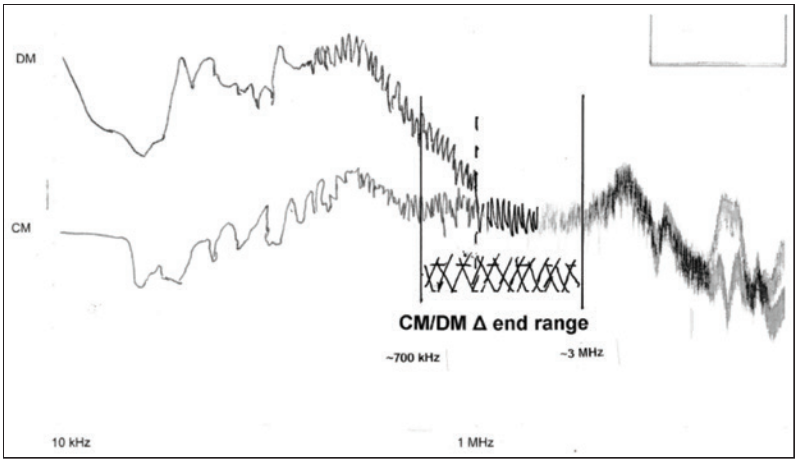

Figure 2: Frequency domain conducted emissions from VSD units annotated

frequency triangular waveform which is a non-sinusoidal waveform.

In this analysis, the assumption is that the Device Under Test (DUT) driven by a non-sinusoidal waveform capacitively couples some of this waveform into earth/ground which becomes the input for this analysis. The analysis shows the IEC Touch Current test circuit (Figure 4 lower circuit diagram and SPICE input conditions) used to capture this electric shock component to determine whether the residual current in the earth/ground lead is acceptable for electric shock protection as discussed earlier.

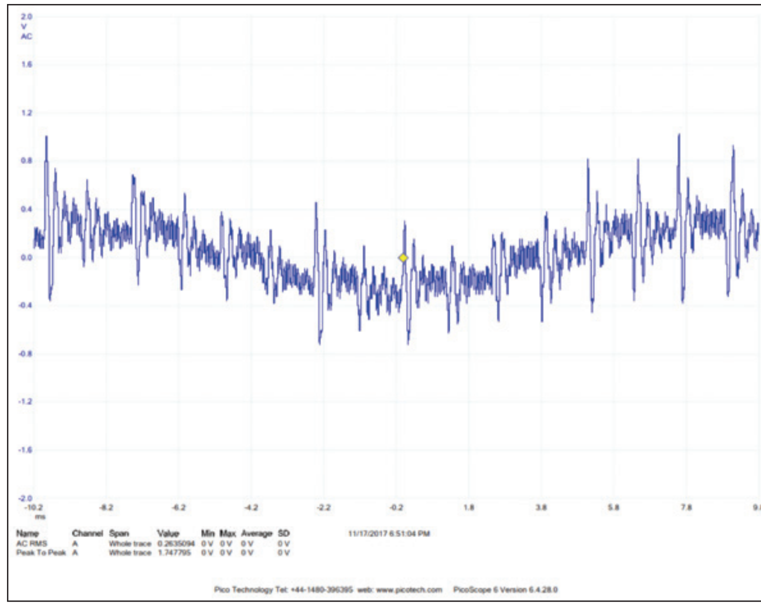

Figure 3: Time domain touch current from a VSD unit

The triangular waveform in the upper part of Figure 4, the blue Input waveform, is the earth/ground complement of the Differential Mode current used by a GFCI to determine when to open the circuit. The red Output/500ohm Touch Current waveform is the Dalziel inverse filtered waveform used to determine whether or not the Touch Current is below the Dalziel letgo-immobilization limit of 7mApk (this method of measurement conveniently reduces the measurement in a way that outputs a value which allows the low frequency Dalziel value to be used for comparison).

Note that the Input current and the Touch Current (= voutput/500ohms) waveforms look quite similar.

The FFT frequency components of the Input waveform are show in Figure 5.

The FFT frequency components of the Touch Current are shown in Figure 6. As can be seen, the low frequency components of the current are not significantly changed by the filter; at about 10kHz the inverse Dalziel Filter Factor filters the output current which is reduced in value moving up to 1MHz. The high frequency components above 10kHz are reduced accordingly and are a small value compared to the Input current values.

Finally, note that for each FFT waveform a little more than half of the total current value is contained in the fundamental (first harmonic) peak.

For this simple waveform example there is a monotonic decrease of current as the frequency increases. Contrast this to Figure 2 DM current which does not exhibit the same type of behavior.

RESULTS

The **frequency domain conducted emissions** are shown in Figure 2. For one product, the full set of data is displayed and, for the other two units, the plot is annotated to illustrate the range of frequencies where the CM (Common Mode) and DM (Differential Mode) signals come together indicating that there is no significant difference showing escaping

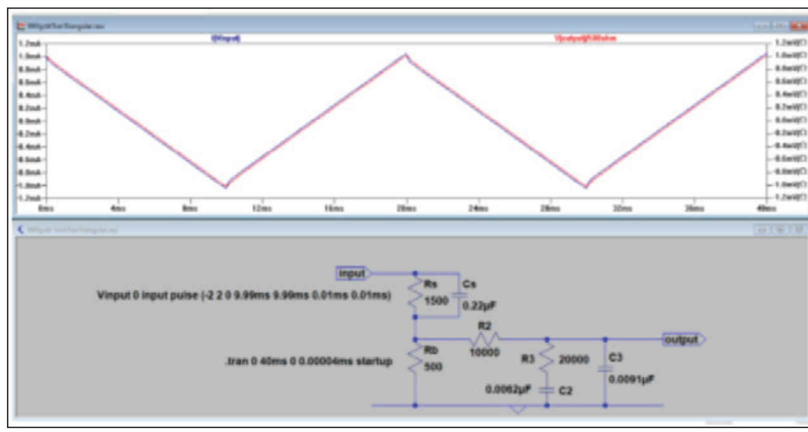

Figure 4: Line frequency triangular waveform analysis

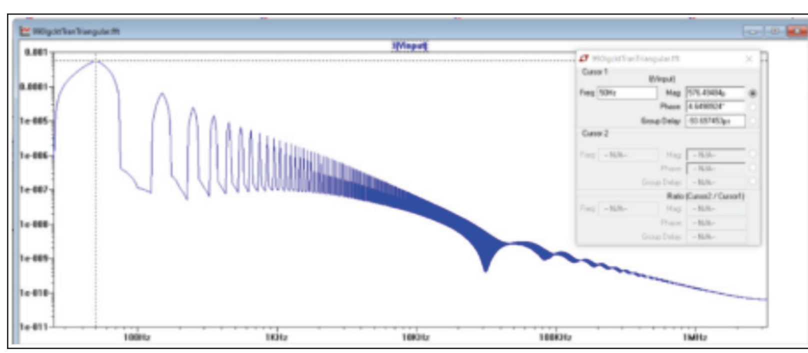

Figure 5: Input current FFT

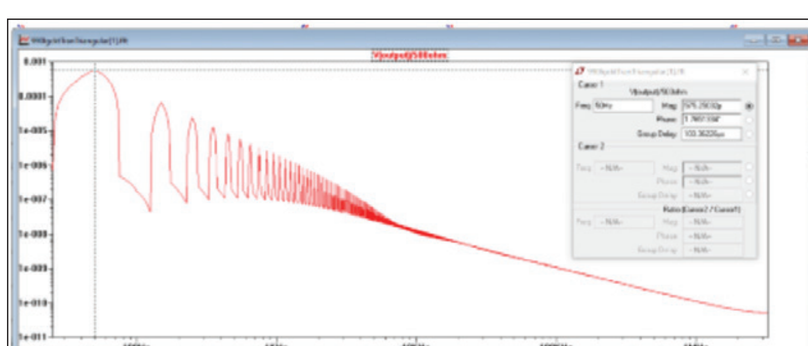

Figure 6: inverse Dalziel filtered Touch Current FFT

current above this frequency. This unique presentation (a feature of this paper) is a combined comparison of two separate data runs showing the CM and DM plots overlaid; the low frequency data for the full dataset has been hand enhanced from the original scans as they were hardly readable (enhancement simplified, does not fully follow the twists and turns). Note that the DM current is the inverse of the touch current measured in the earth/ground lead as described earlier. Also note that the scan starts at 9kHz; below a 10kHz start for some common EMC measurements.

Also note that the scans merge in the range of 1 MHz or so, which applies to all of the units tested; however, there is plenty of HF signal remaining above the 1MHz frequency.

1MHz is mentioned as this is the historic or traditional division of responsibility between product safety and EMC requirements. However, this division is being abrogated going both directions as with the introduction of many high frequency switching devices into products and increased concern for technical interference at lower frequencies.

The DM conducted emissions feeding back into the powerline provide the signal evaluated by the GFCI to determine when to open the line to prevent an electric shock to a user contacting the equipment in a grounded environment. The GFCI uses the DM signal as a proxy for the touch current, assuming all the missing current is going to ground, most likely through a person.

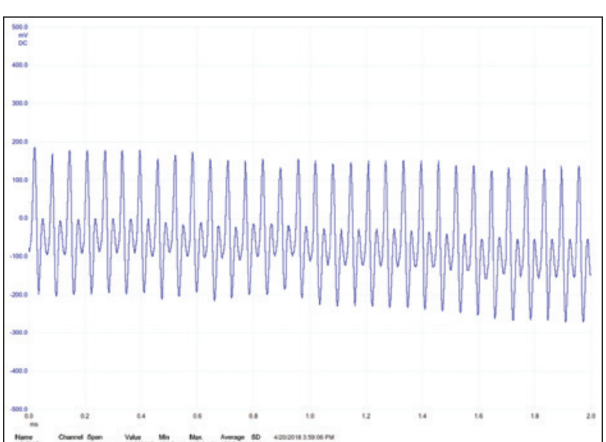

Figure 7: Time domain touch current from programmed VSD unit

The **time-domain touch current** in the earth/ground lead for the NORMAL operating condition is shown in Figure 3. There is significant HF content in this waveform; the VSD switching spikes are clearly seen in this plot.

Note that Figures 2 and 3 are complementary in content; the earth/ground touch current has been capacitively shunted into the earth/ground wire from the line current; every filtered current peak in the touch current removes that current peak from the line current.

As reported in the testing carried out for this research, one unit tripped two of the GFCIs under specific test conditions; neither of these GFCIs were the devices reported tripping in the earlier paper [1]. The other units did not trip any of the GFCIs tested, even though the manufacturer submitted them because they had GFCI issues in the field; it was admitted at the end of the project that EMI mitigation had been applied to each of them.

Control of the touch current from the equipment is needed to protect the user from getting an electric shock from the equipment; this is a common equipment safety requirement.

The two programmed units tested changed the VSD drive conditions as the programmed operation continued through its cycle. Figure 8, in the Appendix on page 32, captures one of those cycle changes and it is clear that there is additional high frequency noise developed during the 2nd half of the touch current plot.

CONCLUSIONS

From this study we clearly observe the wide range of high frequency components in the switching signals of VSD driven motors. These conducted emission signals that pose a threat, fed back from units under test into the output of the GFCI protective device, extend well above 1MHz (the traditional division of responsibility between product safety and EMC work).

Both conducted line emissions and the ground wire touch current demonstrate these broad frequency range signals.

The high frequency signals have to be taken into account to achieve proper control of both the electric shock safety as well as the equipment performance on the power grid. These broadband signals pose threats by interacting with the GFCI protection circuit, but, since they are not expected, they are not specifically evaluated as to whether or not they exceed the Dalziel letgo-immobilization limit as expanded by the known Frequency Factory to high frequency. This phenomenon gives rise to this unexpected result, nuisance tripping of GFCIs, which is a technical problem that needs to be clearly investigated and for which this paper provides substantial data to further pursue this investigation.

Finally, it is important to point out that the conducted emissions feedback issue is not an isolated problem in any way. The referenced paper by LeFrink [5] provides a good history of the development of Conducted Interference Challenges within Europe and discusses cases similar to those discussed in this paper. The paper by Zheng and He [6] describe the analysis of a SMPS circuit looking at the CM and DM conducted emissions, as presented in this paper, showing that it is a serious enough issue to the Chinese development of consumer and commercial equipment that reinforces that this study is important.

REFERENCES

1. Matthew S. Yuen, Student Member, IEEE, Jacob P. Kirby, Student Member, IEEE, Peter E. Perkins, Life Fellow, IEEE, Aziz S. Inan, Senior Member, IEEE, and Henry W. Benitez, Senior Member, IEEE; Why Do GFCIs keep tripping; IEEE PSES ISPCE 2017 Proceedings.
2. Effect of current on human beings and livestock – Part 1: General aspects, IEC 60479-1.
3. C. F. Dalziel, "Effects of Electric Shock on Man," IRE Transactions on Medical Electronics, vol. PGME-5, pp. 44-62, July 1956.
4. R. M. Fish, L. A. Geddes, "Conduction of Electrical Current to and Through the Human Body: A Review," Eplasty, vol. 9, 2009. [Online]. Available: https://www.ncbi.nlm.nih.gov/pmc/articles/PMC2763825
5. Leferink, F; Conductor Interference, Challenges and Interference Cases.pdf; IEEE EMC Magazine, v4, q1 2015.
6. B Zheng, J He; Conducted Emissions Analysis and Suppressions Design of a DC-DC Semi-isolated Power Supply; IEC EMC Symposium 2017 #141-7349.

7. Innovation and Technology Commission. Calibration of Electrical Fast Transient/Burst Generators According to 61000-4-4(ed2):2004. [Online]. Available: http://www.itc.gov.hk/en/quality/scl/doc/scl/rf/rf_talk_burst_10.pdf
8. M. Holt (2002, Mar. 1) How GFCIs Work. [Online]. Available: http://ecmweb.com/content/how-gfcis-work
9. M. Holt (2002, Mar. 1). NEC Requirements for Ground-Fault Circuit Interrupters (GFCI). [Online]. Available: http://ecmweb.com/codebasics/nec-requirements-ground-fault-circuit-interrupters-gfci
10. V. Kraz, "Mitigating EMI Issues in Servo Motors and Variable Frequency Drives" in 2016 EMC Test and Design Guide, pp. 9-16, 2016.
11. Electromagnetic compatibility (EMC) – Part 4-4: Testing and measurement techniques – Electrical fast transient/burst immunity test, IEC 61000-4-4, 2004.
12. S. Hanumanthaiah, S. NVNS. (2016, Aug. 29). Design Considerations for Electrical Fast Transient (EFT) Immunity. [Online]. Available: http://www.cypress.com/file/138636/download
13. Methods of measurement of touch current and protective conductor current; IEC 60990, Ed 3.
14. J. Kimball and J. Henry, "Compatibility between GFCI Breakers and Household Adjustable Speed Drives," 2009 IEEE Energy Conversion Congress and Exposition, San Jose, CA, 2009, pp. 517-520.
15. S. T. Donahue, C. L. Storm, D. A. Wetz, and W. J. Lee, "Study of the Effects of Smart Meter RF Transmissions on GFCI Outlets," in IEEE Transactions on Electromagnetic Compatibility, vol. 56, no. 6, pp. 13611369, Dec. 2014.

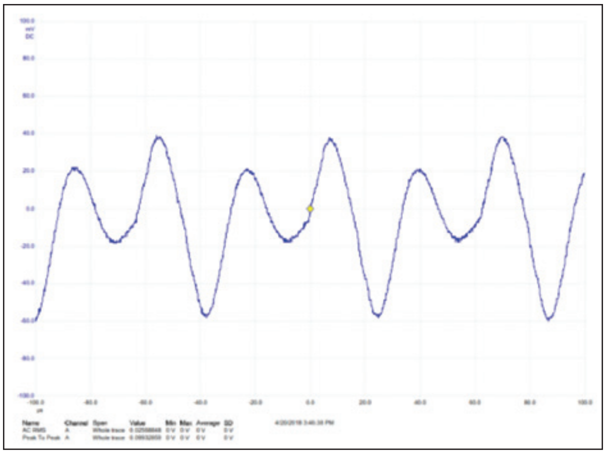

Figure 8: touch current curve, example A

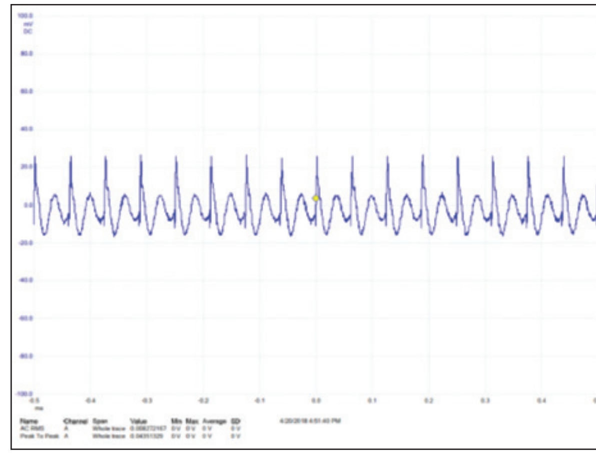

Figure 9: touch current curve, example B

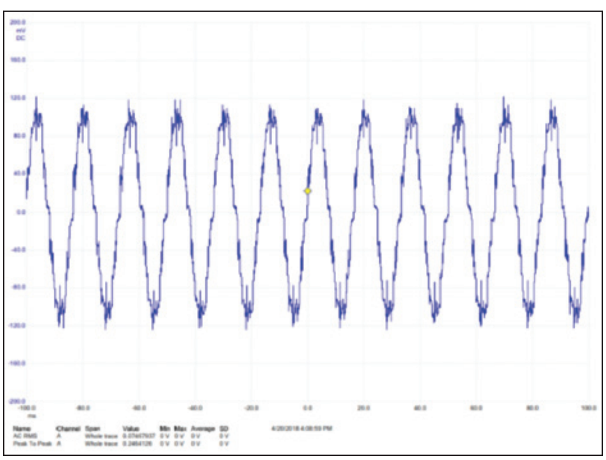

Figure 10: touch current curve, example C

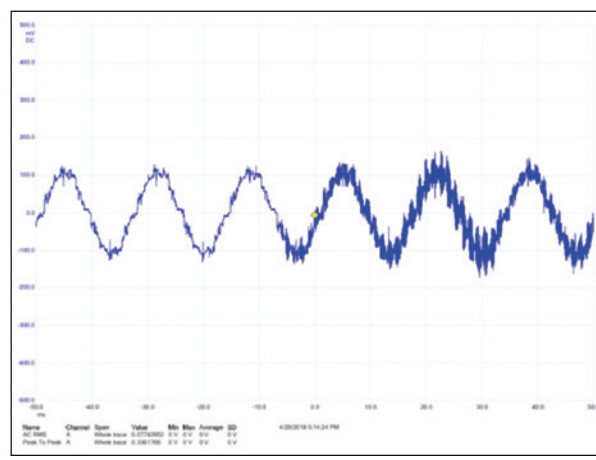

Figure 11: touch current curve, example D

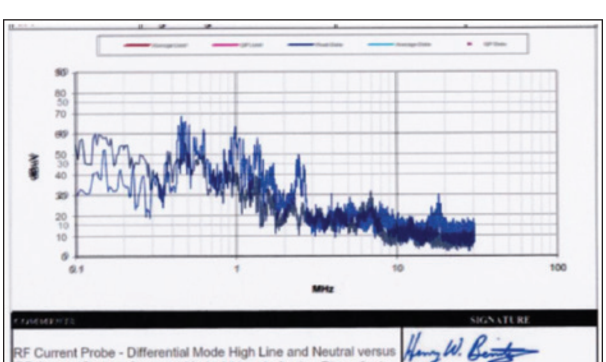

Figure 12: Frequency domain conducted emissions combined, example 1

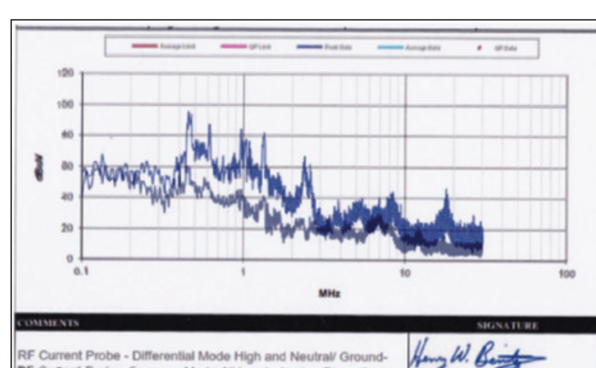

Figure 13: Frequency domain conducted emissions combined, example 2

APPENDIX A: VARIATIONS SEEN IN PROGRAMMED MACHINES

The programmed appliances worked through their cycles based upon an internal schedule.

Touch Current Variations

Even though the testing process was searching for the worst-case touch current, the machines could not be held in any specific cycle for testing. The cycle steps were, by and large, long enough that the touch current reading could be taken however.

The touch current examples shown here present the broad range of touch current seen from two similar programmed machines.

The cases that represented the worst cases were presented earlier.

Figure 11 shows the variation in the touch current as the cycle changes in the machine. The latter part of the trace has considerably more HF content than the earlier cycles.

Combined CM and DM EMI Curves

For the EMI testing, the operating cycle steps were short compared to the testing time. The data of Figure 2 plus Figures 12 and 13 here is then combined into a single curve incorporating the changes due to the operating cycle of the equipment.

The point at which these two curves come together represent the point where the differences are disappearing between the two effects.

Both of these units had frequency response similar to the other unit tested, even though some EMI mitigation had been applied.

EVERYTHING YOU NEED TO KNOW ABOUT EV Battery and BMS Testing in Validation and Production Scenarios

An Overview of Battery Pack Design and Testing Considerations

Electric vehicles are clearly a rapidly growing part of the automotive scene. They promise low or no emissions, conceivably low cost of energy from the power grid, yet they will continue to deliver us safely from here to there. However, electric vehicle design and manufacturing is clearly a paradigm shift for the automotive industry – new drive systems, technologies, and test plans.

Electric vehicles are bringing new test and validation challenges as the electronic and software content of the vehicles grow. In this article, we will discuss the basics of electric vehicle battery pack designs and some of the tests that should be performed on them in a manufacturing environment. We'll also discuss a conceptual solution to this complex testing challenge.

THE MOTIVATION FOR EV BATTERY TESTING

The battery packs used as the rechargeable electrical storage system (RESS) in electric vehicles (EVs), hybrid electric vehicles (HEVs), and plug-in hybrid electric vehicles (PHEVs) are large and complex. Controlled release of the battery's energy provides useful electrical power in the form of current and voltage. Uncontrolled release of this energy can result in dangerous situations such as release of toxic materials (i.e. smoke), fire, high pressure events (i.e. explosions), or any combination thereof.

Uncontrolled energy releases can be caused by severe physical abuse, such as crushing, puncturing, or burning, which can be mitigated by mechanical safety systems and proper physical design. However, they can also be caused by shorted cells, an abnormally high discharge rate, excessive heat buildup, overcharging, or constant recharging, which can weaken the battery. These causes are best prevented by a properly designed and validated electronic safety and monitoring system, better known as a battery management system (BMS).

One of the major validation and safety challenges to be tackled in modern EVs, HEVs, and PHEVs

Brent Hoerman is a Project Manager at DMC and can be reached at brent.hoerman@dmcinfo.com.

Jesse Batsche is a Project Director at DMC and can be reached at jesse.batsche@dmcinfo.com.

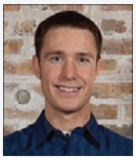

By Brent Hoerman and Jesse Batsche

concerns the effective testing of the Battery Pack itself and the Battery Management Systems (BMS) – the complex electronic system that manages the performance and safety of the battery pack and the high levels of electrical energy stored within. In the sections below, we will describe both the battery pack and the BMS in greater detail.

INSIDE AN EV BATTERY PACK

Battery pack designs for EVs are complex and vary widely by manufacturer and specific application. However, they all incorporate combinations of several simple mechanical and electrical component systems that perform the pack's basic required functions.

Cells and Modules

Battery cells can have different chemistries, physical shapes, and sizes as preferred by various pack manufacturers. However, the battery pack will always incorporate many discrete cells connected in series and parallel to achieve the pack's total voltage and current requirements. In fact, battery packs for all electric drive EVs can contain several hundred individual cells.

The large stack of cells is typically grouped into smaller stacks called modules to assist in manufacturing and assembly. Several of these modules will be placed into a single battery pack. The cells are welded together within each module to complete the electrical path for current flow. Modules can also incorporate cooling mechanisms, temperature monitors, and other devices. In most cases, modules also allow for monitoring the voltage produced by each battery cell in the stack by the BMS.

Safety Components and Contractors

Somewhere in the middle, or at the ends, of the battery cell stack is a main fuse that limits the pack's current under a short circuit condition. There is also commonly a service plug or service disconnect located somewhere within the battery stack's electrical path, which can be removed to split the battery stack into two electrically isolated halves. With the service plug removed, the exposed main terminals of the battery present reduced electrical danger to service technicians. A high voltage interlock circuit will often run throughout key elements and connection points of the pack to establish hard-wired safety functions.

The battery pack also contains relays, or contactors, which control the battery pack's electrical power distribution to the output terminals. In most cases, there will be a minimum of two main relays that connect the battery cell stack to the pack's main positive and negative output terminals, those supplying high current to the electrical drive motor. Some pack designs will include alternate current paths for pre-charging the drive system through a pre-charge resistor or for powering auxiliary busses with their associated control contactors. For obvious safety reasons these contactors are all normally open.

Temperature, Voltage, and Current Sensors

The battery pack also contains a variety of temperature, voltage, and current sensors. At least one main current sensor will measure the current being supplied by, or sourced to, the pack. The current from this sensor can be integrated to track the actual state of charge (SoC) of the battery pack. The state of charge is the pack capacity expressed as a percentage and can be thought of as the pack's fuel gauge indicator. The battery pack will also have a main voltage sensor, for monitoring the voltage of the entire stack and a series of temperature sensors, such as thermistors, located at key measurement points inside the pack.

Collection of data from the pack sensors and activation of the pack relays are accomplished by the pack's battery management system (BMS). The BMS is also responsible for communications with the world outside the battery pack and performing other key functions, as described in the following section.

INSIDE AN EV BATTERY MANAGEMENT SYSTEM (BMS)

The BMS controls almost all electronic functions of the EV battery pack, including battery pack voltage and current monitoring, individual cell voltage measurements, cell balancing routines, pack state of charge calculations, cell temperature and health monitoring, ensuring overall pack safety and optimal performance, and communicating with the vehicle engine control unit (ECU).

In a nutshell, the BMS system must read voltages and temperatures from the cell stack and inputs from associated temperature, current, and voltage sensors. From there, the BMS must process the inputs, make logical decisions to control pack performance and safely, and report input status and operating state through a variety of analog, digital, and communication outputs.

BMS TOPOLOGY

Modern BMS systems for EV applications are typically distributed electronic systems. In a standard distributed topology, routing of wires to individual cells is minimized by breaking the BMS functions up into at least two categories. The monitoring of the temperature and voltage of individual cells is done by a BMS sub-module board, which is mounted directly on each battery module stack. Higher level functions such as computing state of charge, activating contactors, etc. along with aggregating the data from the sub modules and communicating with the ECU are done by the BMS main module.

The sub-modules and main module communicate on an internal data bus such as controller area network (CAN). Power for the BMS can be supplied by the battery stack itself or from an external primary battery such as a standard 12V lead acid battery. In some cases, the main module is powered externally, while the sub modules are powered parasitically from the battery modules to which they are attached.

BMS STATE OF CHARGE CALCULATION

The BMS is responsible for tracking a battery pack's exact state of charge (SoC). This may simply be for providing the driver with an indication of the capacity left in the battery (fuel gauging), or it could be used for more advanced control features.

For example, SoC information is critical to estimating and maintaining the pack's usable lifetime. Usable battery life can be dramatically reduced by simply charging the pack too much or discharging it too deeply. The BMS must maintain the cells within safe operating limits. The SoC indication is also used to determine the end of the charging and discharging cycles.

To measure SoC the BMS must include a very accurate charge estimator. Since you can't directly measure a battery's charge, the SoC must be calculated from measured characteristics like voltage, temperature, current, and other proprietary (depending on the manufacturer) parameters. The BMS is the system responsible for these measurements and calculations.

BMS CELL BALANCING FUNCTIONS

The BMS must compensate for any underperforming cells in a module, or stack, by actively monitoring and balancing each cell's SoC. In multi-cell battery chains, small differences between cells (as a result of production tolerances, uneven temperature distribution, intrinsic impedance, and/or aging characteristics) tend to be magnified with each charge and discharge cycle. In EV applications the number of cycles can be very high due to the use of regenerative braking mechanisms.

When degraded cells with a diminished capacity exist within the battery stack, the performance of the pack as a whole is degraded. During the charging cycle, there is a danger that degraded cells would be subject to overcharging before the rest of the cells in the chain reach their full charge. As a result, temperature and pressure may build up and possibly damage that cell. The weakest cell will have the greatest depth of discharge during discharging and will tend to fail before the others. The voltage on the weaker cells could even become reversed as they become fully discharged before the rest of the cells resulting in the early failure of the cell.

Cell balancing is an active way of compensating for weaker cells by equalizing the charge on all the cells in the chain and thus extending the battery pack's usable life. During cell balancing, circuits are enabled which can transfer charge selectively from neighboring cells, or the entire pack, to any undercharged cells detected in the stack.

To determine when active cell balancing should be triggered and which target cells, the BMS must be able to measure the voltage of each individual cell. Moreover, each cell must be equipped with an active balancing circuit.

STATE OF HEALTH AND DIAGNOSTICS

The state of health (SoH) is a measure of a battery's capability to safely deliver its specified output. This metric is vital for assessing the readiness of the automobile and as an indicator of required maintenance.

SoH metrics can be as simple as monitoring and storing the battery's history using parameters such as number of cycles, maximum and minimum voltages and temperatures, and maximum charging and discharging currents, which can be used for subsequent evaluation. This recorded history can be used to determine whether it has been subject to abuse, which can be an important tool in assessing warranty claims.

More advanced measures of battery SoH can include features such as automated measurement of the pack's isolation resistance. In this case, specialized circuits inside the battery pack can measure the electrical isolation of the high current path from the battery pack ground planes. Such a safety system could preemptively alert the operator or maintenance technicians to potential exposure to high voltage.

BMS COMMUNICATIONS

Most BMS systems incorporate some form of communication with the world outside the battery pack, including the ECU, the charger controller, and/or your test equipment. Communications interfaces are also used to modify the BMS control parameters and for diagnostic information retrieval.

CAN (controller area network) is the most common communications bus in automotive applications, although automotive ethernet, RS232 / RS485 serial, SPI, TCP/IP, or other networks could be used. CAN networks come in various implementations and can include a range of higher level “application layer” protocols like unified diagnostic services, OBD II, J1939, etc.

Aside from a digital bus, separate analog and/or digital inputs and outputs should be considered as supplemental parts of the BMS interface and communication. Discrete inputs and outputs can be used for redundancy and for operations requiring a separate interface such as activating an external contactor, fan, or dashboard lamp.

TESTING AN EV BATTERY PACK

Developing a test strategy for an assembly as large, complex, and powerful as an EV battery pack can be a daunting task. Like most complex problems, breaking the process down into manageable pieces is the key to finding a solution. Accordingly, testing only at carefully selected points in the development and manufacturing process will reduce the effort required. These key points for many pack manufacturers include BMS development, pack development, module production, and pack production. What tests are performed at each step is a different matter altogether and depends on the specifics of the process and the device.

BMS Development Testing

During BMS Development, engineers need a way to reliably test the BMS under real-world conditions to complete their verification and validation plans. Test strategies such as hardware-in-the-loop (HIL) testing are often performed at this stage. HIL testing involves simulating physical inputs and external connections to the pack while monitoring its outputs and behavior relative to design requirements.

Accurately simulating all the conditions to which a BMS may be subjected during real world operation is not easy. However, one must consider the long-term cost of skipping testing over a full range of conditions, remembering that any given condition could lead to a critical failure in the field. In the end, simulating nearly every combination of cell voltages, temperatures, and currents you expect your BMS to encounter is really the only way to verify that your BMS reacts as you intended in order to keep your pack safe and reliable.

Pack Development Testing

At the pack development stage, engineers are typically concerned about testing the entire assembly through various types of environmental stress testing as part of design validation or product validation plans. Environmental stress could include exposure to temperature extremes, thermal shock cycling, vibration, humidity, on-off cycling, charge discharge cycling, or any combination of these. The testing requirements here typically include performing a full batch of performance tests on a pack both before and after application of the stress. Live monitoring of the pack throughout the environmental stress period may also be required.

Module Production Testing

Requirements for module level testing vary widely depending on the actual design of the system. The main testing to be done at this point involves simple charge/discharge testing to ensure that connections between cells are robust and can handle the intended current loads without failing or shedding excessive

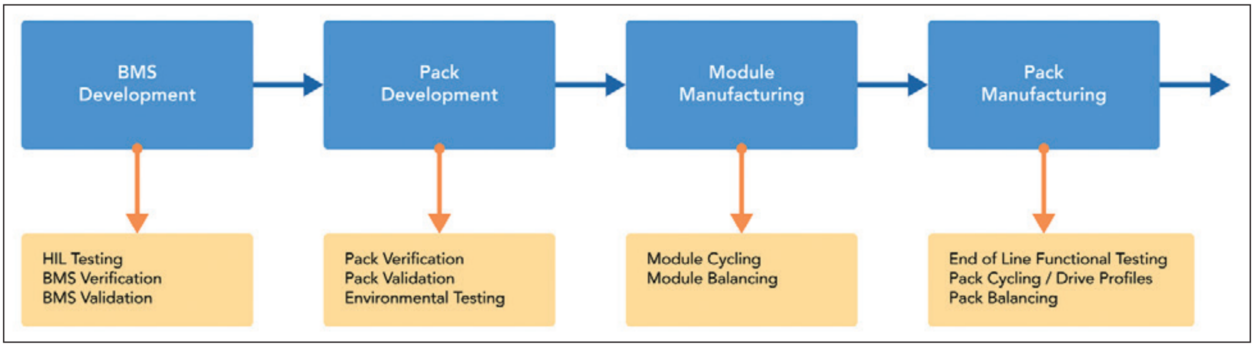

Figure 1: EV battery pack test sequencing

heat. Further testing could involve ensuring the cell voltages are reported correctly, that the cells are balanced, and/or that the cooling and temperature monitoring sensors are working properly.

Pack Production Testing

Pack level testing is done after the pack has completed, or is at least very close to, the point of final assembly, or end of line (EOL). At this stage, the pack must complete a full batch of tests to ensure proper functioning of every major pack subsystem (functional testing). These tests include simple pinout and continuity checks, confirming proper relay operation, testing functionality of safety devices such as high voltage interlocks, carefully measuring the isolation resistance under high potential (hi-pot testing), and testing proper communications and operation of the BMS.

After EOL functional testing is completed, packs may also be subjected to charge/discharge cycling and drive profile cycling, which will simulate the typical conditions the pack will see when integrated into the EV drivetrain. Packs can also be run through active cell balancing routines to set each cell's initial charge state to a nominal condition or set the Pack SoC to a level appropriate for shipping and storage.

EV BATTERY PACK TESTING SOLUTIONS

Once you have decided where you are testing and what you are testing, you need to determine how you will be testing. Since every battery pack design has unique elements, and since testing requirements vary accordingly based on agreements between the manufacturer and end user, in reality, there is no one-size-fits-all solution for everyone's battery pack testing needs.

Off-the-Shelf Testing Solutions

That being said, some portions of the testing, such as charge/discharge/drive cycle evaluation, are standardized. As such, pre-packaged, off-the-shelf hardware and software solutions exist for these particular test steps. These systems typically use only the positive and negative output terminals, as these are the only elements common to every battery pack. These turn-key systems may even allow you to add in options required to test components and functions specific to your battery pack, such as CAN communications, external relay activation, etc.

When considering off-the-shelf systems for use in your test plan, make sure to ask yourself these three basic questions:

1. Are you getting everything you need just the way you want it, or are you settling for what the other person needs?

2. Are you using everything you will pay for, or are you paying for things you won't use?
3. Is it flexible enough to accommodate your future needs but not so flexible that it becomes cumbersome to use?

Arguments for a Customized, Modular Test System Approach

Building a functional test system tailored to your battery pack and your specific testing needs often sounds like a more costly and time-consuming approach, and it can be. However, the route you take to achieve that end goal makes a world of difference in the outcome and in long-term ROI.

Choosing a modular hardware and software testing platform tailored to meet your requirements can be used to jump start this approach, making it a very viable option. This is especially true if the platform you choose leverages proven commercial technologies and open industry standards.

In the end, this modular platform-based testing approach can have several benefits:

1. It can dramatically lower the cost of the test system, both in initial capital expenditure and overall cost of ownership, through the use of commercial technologies and standards.
2. It can increase your test throughput with fast measurement hardware and software capable of managing multiple test routines in parallel.
3. The time required to adapt such test systems for new products will decrease through the use of flexible, modular software and hardware.
4. You can get exactly what you need, the way you want it. You can get everything you paid for and your test station will be flexible, without being cumbersome to use.
5. The system is tailored to your product and workflows, resulting in a simplified user experience, shorter learning curve, and corresponding personnel time savings.

A PLATFORM APPROACH

The preceding sections describe the challenging problem statement of thoroughly testing a complex, high power system like an EV battery packs and BMS.

It is highly desirable to achieve standardization, cohesion, and efficiency of testing throughout the EV component product cycle and during inevitable future product evolution. It is best to take a platform-based approach to address this testing challenge to achieve this. This means establishing a unified suite of test equipment built on common reusable building blocks (both hardware and software) and utilizing various configurations of this platform to cover testing of battery cells, modules, packs across various testing regimes (R&D, validation, HIL, production, and lifecycle tests).

This requires incorporating reliable software and hardware architectures and flexible and reliable subsystem components, which can be customized to specific use cases and changing requirements. Utilizing high-quality COTS (commercial off-the-shelf) hardware assembled from best-in-class instrumentation vendors typically improves system performance, reliability, and maintainability while significantly reducing the engineering effort involved in deploying the system.

CONCLUSION

Battery packs used in today's EVs are complex systems designed to provide safe and efficient electrical power. As such, a comprehensive testing strategy to evaluate possible safety and performance considerations is essential to the battery pack manufacturing process. However, testing requirements often vary from manufacturer to manufacturer and from one battery design to another, further complicating the testing process. Using a customized modular test system can be an efficient, cost-effective approach to conducting necessary battery pack testing in a manufacturing environment.

PRODUCT Showcase

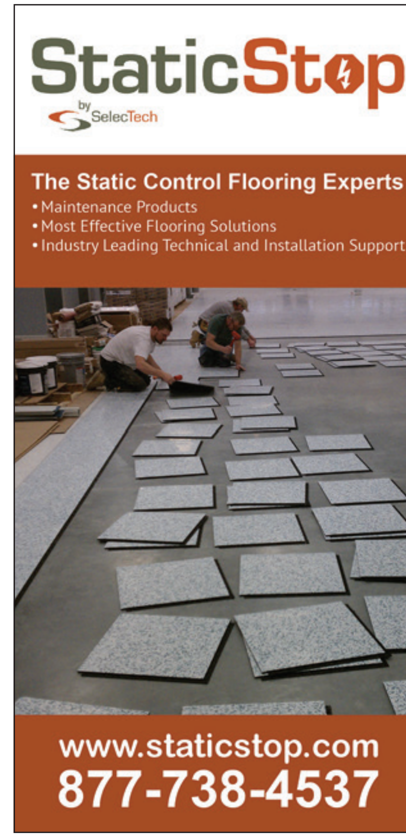

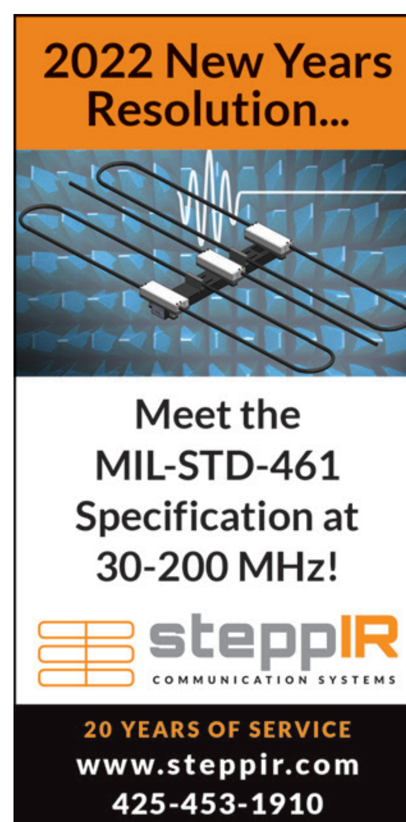

EVALUATION OF EMC EMISSIONS AND GROUND TECHNIQUES ON 1- AND 2-LAYER PCBs WITH POWER CONVERTERS

Part 9: AC/DC Converter – EMC Countermeasures – Conducted and Radiated Emissions Results

By Bogdan Adamczyk, Scott Mee, and Nick Koeller

***Author's Note:** This month's column is Part 9 of our ten-part series devoted to the design, test, and EMC emissions evaluation of 1- and 2-layer PCBs that contain AC/DC and/or DC/DC converters and employ different ground techniques [1-8]. In this part, we continue to focus on the AC/DC power converter board (2-layer PCB). We evaluate the implementation of several EMC countermeasures and present the conducted and radiated emissions results performed according to the CFR Title 47, Part 15, Subpart B, Class B.*


Dr. Bogdan Adamczyk is professor and director of the EMC Center at Grand Valley State University (http://www.gvsu.edu/emccenter) where he regularly teaches EMC certificate courses for industry. He is an iNARTE certified EMC Master Design Engineer. Prof. Adamczyk is the author of the textbook "Foundations of Electromagnetic Compatibility with Practical Applications" (Wiley, 2017) and the upcoming textbook "Principles of Electromagnetic Compatibility with Laboratory Exercises" (Wiley 2022). He can be reached at adamczyb@gvsu.edu.


Scott Mee is a co-founder and owner at E3 Compliance which specializes in EMC & SIPI design, simulation, pre-compliance testing and diagnostics. He has published and presented numerous articles and papers on EMC. He is an iNARTE certified EMC Engineer and Master EMC Design Engineer. Scott participates in the industrial collaboration with GVSU at the EMC Center. He can be reached at scott@e3compliance.com.


Nick Koeller is an EMC Engineer at E3 Compliance which specializes in EMC & SIPI design, simulation, pre-compliance testing and diagnostics. He received his B.S.E in Electrical Engineering from Grand Valley State University and is currently pursuing his M.S.E in Electrical and Computer Engineering at GVSU. Nick participates in the industrial collaboration with GVSU at the EMC Center. He can be reached at nick@e3compliance.com.

1. INTRODUCTION

In Part 8, we evaluated the performance of the baseline AC/DC converter. The baseline AC/DC converter had only the components needed for functionality and did not have any specific EMC components populated. The results showed multiple failures in both radiated and conducted emissions.

Here, we present a systematic approach to improve these failures by populating the PCB with optional EMC countermeasures on component pads that have already been designed into the PCB layout and show their impact on the radiated and conducted emissions. The EMC countermeasures are illustrated in Figure 1 as purple dashed boxes labeled EMC-A through EMC-F.

We'll first look at conducted emissions results, followed by radiated emissions results, and conclude with what you can expect in next month's column, Part 10.

2. CONDUCTED EMISSIONS RESULTS

Conducted emissions were measured in the frequency range of 150 kHz – 30 MHz. The conducted emissions results show multiple failures up to the frequency of 20 MHz, as shown in Figure 2a. The failures are comprised of the fundamental switching frequency (~ 270kHz) and the subsequent harmonics.

In an attempt to reduce these emissions, we began with the front-end filtering components (EMC-A) such as Y-capacitors (C13, C17) of the value 0.022µ, between line (L-Filter) and protective earth (PE), and neutral (N_Filter) and PE and an X-capacitor (C15) of the value 0.1µF, between the line and neutral.

The conducted emissions measurement taken with these countermeasures populated is shown in Figure 2b.

As the plot in Figure 2b shows, the capacitors decrease the emissions by 4-15 dB, over the entire frequency range. There was only one quasi-peak failure at

255 kHz (still reduced by about 5 dB from baseline). There are still several failures over a broad range of frequencies when measured with the average detector.

Next, a Schaffner RN112-0.5-02-27M common-mode choke (L3) was added. The results are shown in Figure 3.

The addition of the common-mode choke eliminated the quasi-peak failure and lowered the emissions mainly below 1 MHz. It may be possible with further study to reduce conducted emissions by evaluating different common-mode chokes. However, we chose to focus on other EMC design controls to make further reductions.

Next, a 100 Ω gate resistor (R9) for Q1 (switching MOSFET) was added (EMC – C). The results are shown in Figure 4.

The main impact of the gate resistor was above 1 MHz, resulting in a 2-5 dB reduction in emissions. Further adjustments to the gate resistor R9 or R14

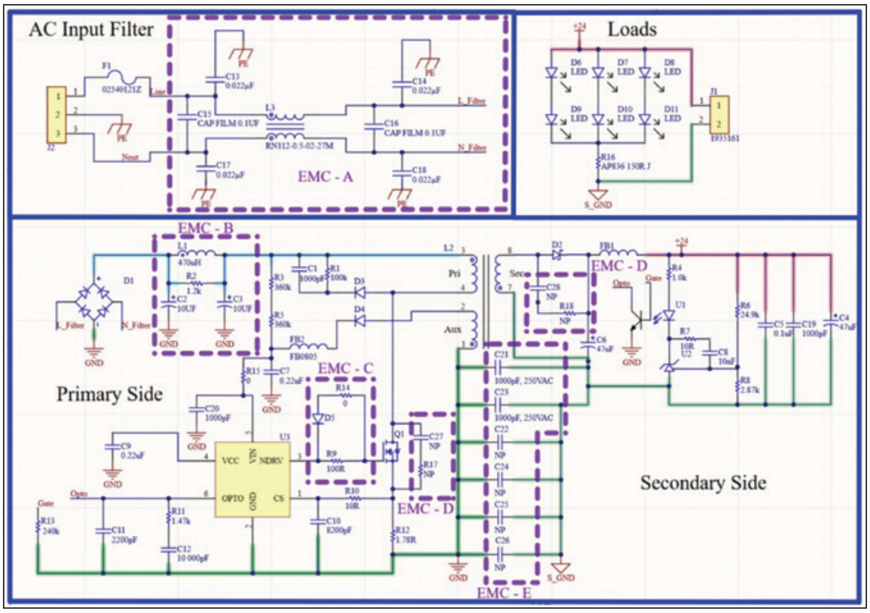

Figure 1: AC/DC schematic with EMC countermeasures

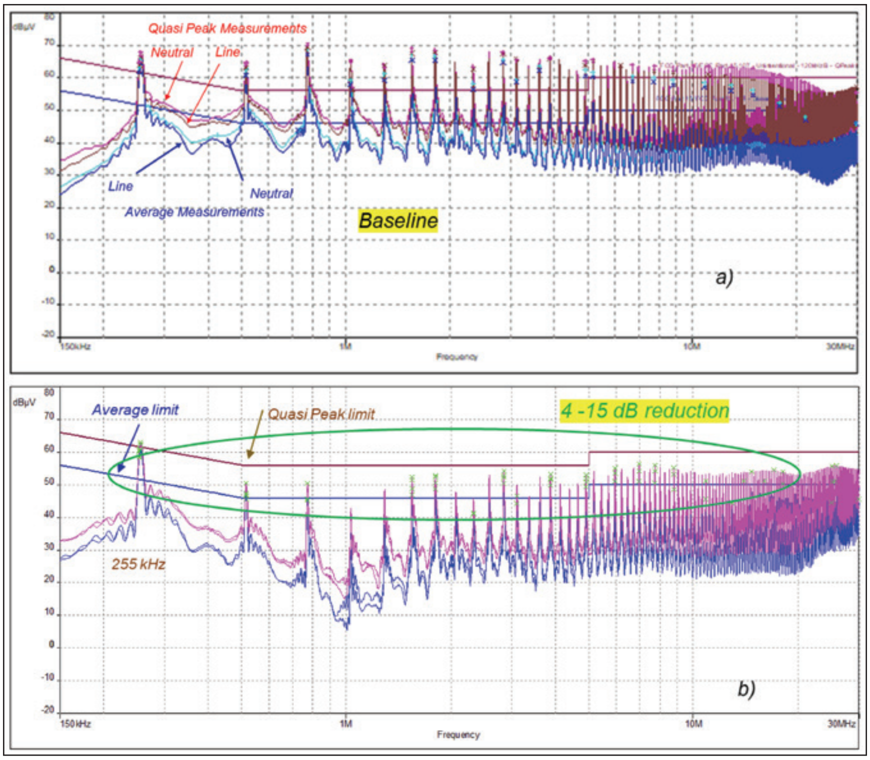

Figure 2: Conducted emissions results: a) baseline b) with X cap (C15 = 0.1uF) & Y caps (C13 = C17 = 22nF)

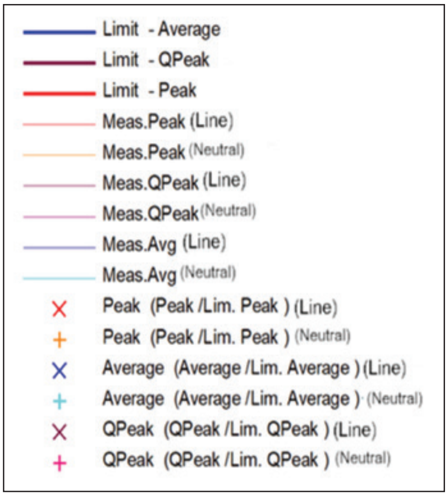

Conducted emission results legend

were not evaluated in conducted emissions, pending the measurements of radiated emissions.

Next, the Y capacitor values (C13 & C17) were increased from 0.022 µF to 0.033 µF (EMC-A). The results are shown in Figure 5.

This change eliminated the remaining conducted emissions failures.

3. RADIATED EMISSIONS RESULTS

Radiated emissions were measured in the frequency range of 30 - 300 MHz. As we have already identified the countermeasures that need to be added to resolve conducted emissions failures, we start radiated emissions diagnostics with all of the required CE modifications populated as per Figure 5. Figure 6a shows the baseline results (DUT with the conducted emissions modifications).

In order to reduce the failing emissions further, two stitching caps (EMC – E) C21 and C23 of the value 1000 pF were added. The stitching capacitors tie the secondary back to the primary at high frequency, allowing noise currents to return to their source more directly rather than through the air, thus reducing the radiated emissions. The result was the reduction in emission, as shown in Figure 6b.

At this point, failures can still be observed in the vertical emissions between 30MHz – 35MHz, and the margin of the emissions around 35-40MHz and 80MHz isn't sufficient. We typically want to see at least a 6dB margin to the required emissions limit to account for lab-to-lab variation and component/build tolerances. Therefore, a snubber was added across the Drain to Source pin of the switching MOSFET Q1 (EMC – D) consisting of R17 = 10 Ω, C27 = 330 pF

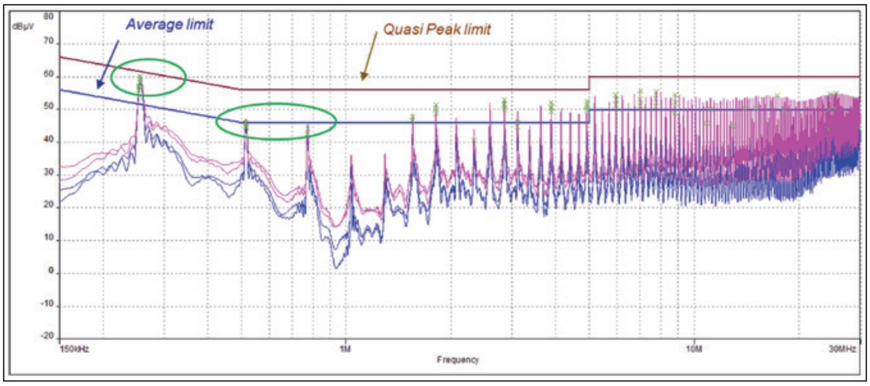

Figure 3: Conducted emissions results: X cap (C15 = 0.1uF) & Y caps (C13 = C17 = 22nF) and CMC (L3 = Schaffner RN112-0.5-02-27M)

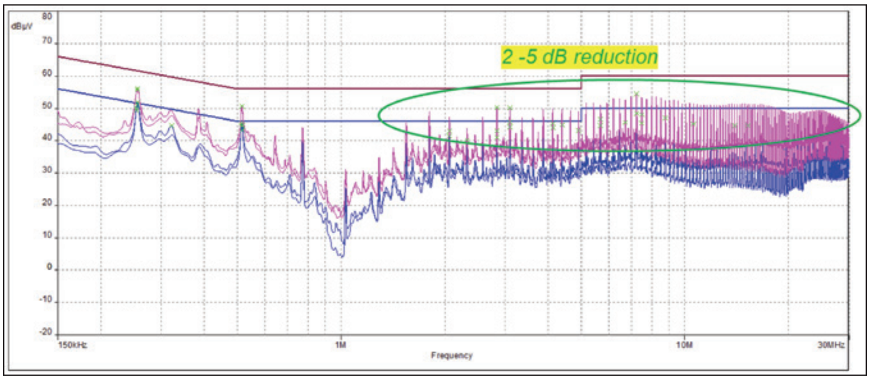

Figure 4: CE results: X cap (C15 = 0.1uF) & Y caps (C13 = C17 = 22nF) CMC (L3 = Schaffner RN112-0.5-02-27M), Gate Drive Resistor (R9=100Ω)

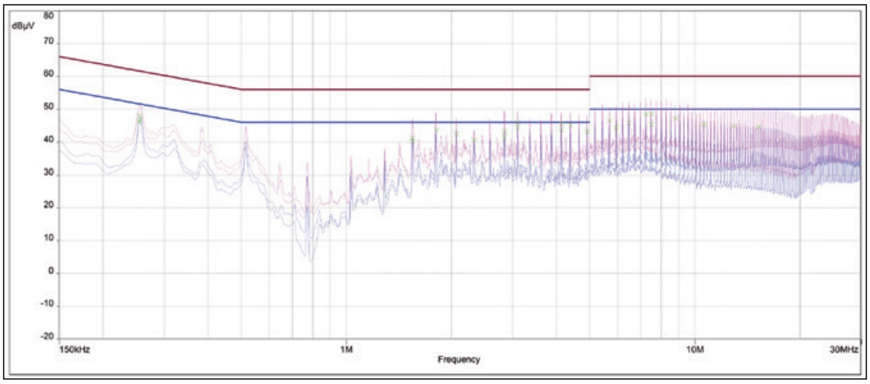

Figure 5: CE results: X cap (C15 = 0.1uF) & Y caps (C13 = C17 = 33nF), CMC (L3 = Schaffner RN112-0.5-02-27M), Gate Drive Resistor (R9=100Ω)

to further reduce the emissions. The results are shown in Figure 7.

The addition of the snubber resulted in the device passing the radiated emission test with sufficient margins. The cumulative changes resulted in passing both conducted & radiated emissions results. Front end filtering through the use of X and Y capacitors along with a common mode choke provided a significant improvement in conducted emissions. Adjusting the Q1 gate resistor, adding a snubber across Q1 Drain-Source and stitching capacitance all made significant improvements in radiated emissions. If further radiated or conducted emissions reductions were needed, some experimentation with R14 (turn off Q1 gate resistance) could be evaluated. All design changes are recommended to be evaluated for potential design trade-offs with other requirements such as thermal power dissipation, functionality over temperature and input voltage variations as well as other EMC requirements (including immunity).

4. FUTURE WORK

Next month's column will focus on three PCB layouts that all have a common schematic (AC/DC converter + DC/DC converter + Digital microcontroller), but different PCB layouts that have the low voltage secondary ground references modified. The conducted and radiated emissions will be evaluated between three GND reference strategies: 1) a single layer ground, 2) two layer ground reference with trace routes on the secondary layer, 3) two layer ground reference with a solid ground plane. The evaluation of these three approaches will help understand the trade offs between ideal and less than ideal GND reference designs.

REFERENCES

1. Adamczyk, B., Mee, S., Koeller, N, "Evaluation of EMC Emissions and Ground Techniques on 1- and 2-layer PCBs with Power Converters," Parts 1-8 available on https://incompliancemag.com.

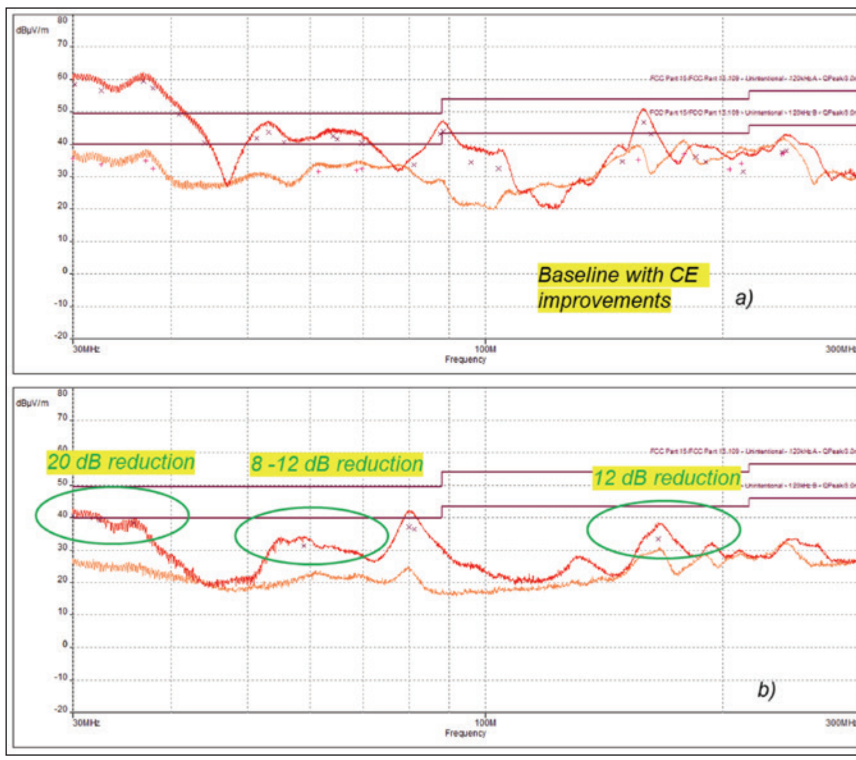

Figure 6: Radiated emissions results: a) baseline with CE modifications b) with added C21 & C23 caps = 1000 pF

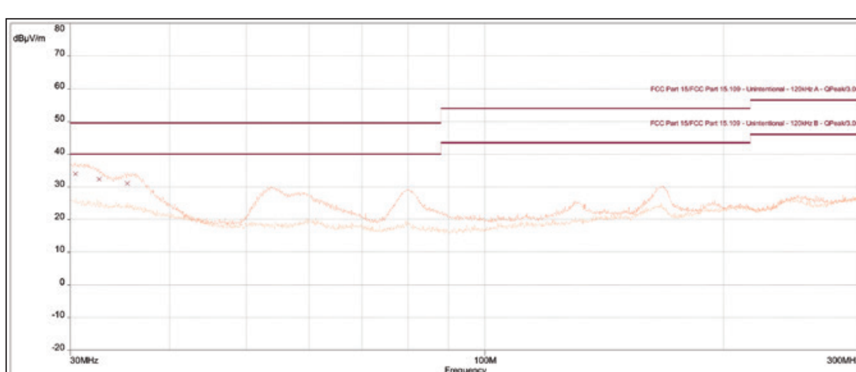

Figure 7: Radiated emissions results with a snubber R17 = 10 Ω, C27 = 330 pF added across switching MOSFET Q1

CHARACTERIZATION FOR ESD DESIGN, THE TLP ZOO: PART 1

By Robert Ashton for EOS/ESD Association, Inc.

Author's Note: *This is the first of a two-part series on the TLP Zoo, the variety of transmission line pulse (TLP) systems used in the characterization of electrical components and system of ESD robustness. In this article, the motivation for TLP measurements will be discussed, followed by TLP basics and the most widely used TLP configuration, time domain reflection (TDR). The second article will cover several alternative TLP configurations, including Kelvin, time domain reflection and transmission and current source TLP, and the importance of a TLP system's load line. The second article will also introduce two extensions of TLP testing that have been proposed for testing integrated circuits for charged device model (CDMJ) robustness as well as present some additional TLP resources.*

Robert Ashton is the Chief Scientist at Minotaur Labs. Robert is an active member of ESDA working groups for device testing standards and the JEDEC latch-up working group. He has been a regular member of the EOS/ESD Symposium technical program committee. Robert served on the ESDA board of directors from 2011 to 2013. He is currently serving as co-chair of the human metal model (HMM) working group.

Founded in 1982, EOS/ESD Association, Inc. is a not for profit, professional organization, dedicated to education and furthering the technology Electrostatic Discharge (ESD) control and prevention. EOS/ESD Association, Inc. sponsors educational programs, develops ESD control and measurement standards, holds international technical symposiums, workshops, tutorials, and foster the exchange of technical information among its members and others.

INTRODUCTION

Electrostatic discharge (ESD) events are high current events that occur over a short period of time. Components such as integrated circuits and electronic systems need to be designed and then tested to ensure that they can survive the ESD events they may experience during their lifetime. Integrated circuits are tested using the human body model (HBM) [1] and charged device model (CDM) [2], while systems are tested using IEC 61000-4-2[3]. A comparison of the waveform characteristics of the three stresses is shown in Figure 1 where stress levels have been adjusted to make the waveform comparisons easier to visualize. HBM involves stress currents on the order of 1 amp with a characteristic length of 150 ns. The waveform in Figure 1 is shown for a 2 kV stress. Today's products are considered ESD robust for handling in an ESD protected area if it passes a 1 kV stress. CDM produces several amps of current lasting on the order of 1 ns. The 4 A stress shown in Figure 1 is a typical stress level for a moderate sized package. The system level stress illustrated in Figure 1 is for a 1 kV stress. Typical stress levels for system level testing are often at 8 kV.

Designing to protect against these levels of stress requires knowledge of device properties at high currents but short times. Producing and measuring such pulse currents and voltages presents a unique challenge. The challenge was answered by Tim

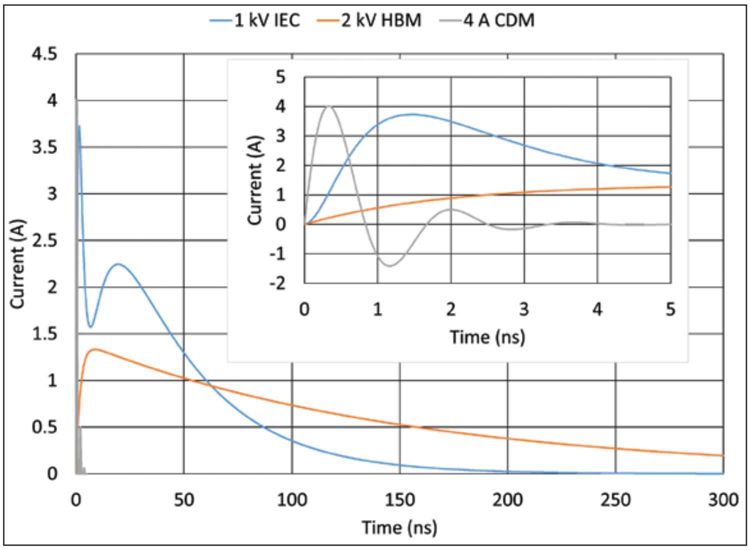

Figure 1: Comparison of ESD test waveforms

Maloney and co-authors in two landmark papers published in 1985 [4][5], the transmission line pulse, TLP, measurement system. With TLP current versus voltage and current and voltage time dependence can be measured in the ESD range of currents and time duration for all three of these ESD stress waveforms. TLP, however, is not just one system, there are a variety of TLP configurations, each with its own advantages and disadvantages. This series will introduce TLP measurement and explore some of the TLP variations in the TLP Zoo.

In the subsequent discussion all coaxial cables are assumed to be 50-ohm cables. It is also important to note that since TLP measurements have both high voltages and currents, it is important to incorporate appropriate attenuators at oscilloscope inputs to prevent damage. For simplicity, these attenuators are not shown. In all figures, current sensors are depicted by an oval around the center conductor and voltage probes are depicted by an arrow with a sense resistor. Connections to the oscilloscope are assumed to be 50-ohm coaxial cables.

THE (OVER) SIMPLIFIED TLP SYSTEM

Figure 2 shows a schematic of a simplified TLP system. TLP works on the principle that a coaxial cable charged to a voltage will produce a square pulse with a current into a short equal to the charging voltage divided by the impedance of the coaxial cable with a duration equal to twice the propagation length of the cable. A 10 m long 50-ohm cable charged to 100 V will produce an approximately 100 ns, 2-amp pulse. Measuring the voltage across the device and the current through the device with appropriate voltage and current probes and a high-speed oscilloscope allows one to determine the current versus voltage characteristics of the device under test (DUT).

Figure 3 illustrates the most common data that is obtained from a TLP measurement, a pulsed I-V curve. Pulses are made with increasing charging voltage and the voltage and current are averaged over a period late in the pulse. Each pulse creates a current versus voltage data point. Plotting the pulses maps out the IV curve. Figure 3 is for a device with snapback characteristics such as a grounded gate nMOS device. For stress voltages below avalanche, breakdown currents are low. Current increases when avalanche breakdown begins. Eventually, avalanche breakdown triggers the nMOS device's parasitic npn device into a non-destructive snapback state. At high enough currents, the device can be damaged, which may be reflected in a second drop in voltage. Most TLP systems include the capability to measure device leakage after each pulse to detect device damage. In this manner, the TLP simultaneously serves as a valuable tool to understand the device physics and the parameters that dictate the snapback behavior.

The system in Figure 2 neglects the effects of multiple reflections which can occur in a TLP system. Unless the DUT has the same impedance as the cable delivering the pulse, usually 50 ohms, there will be reflections that can last for several times the pulse duration. These reflections can damage the DUT at currents well below the DUT's maximum capability, masking the DUT's true capability. For this reason, TLP systems require some method to remove

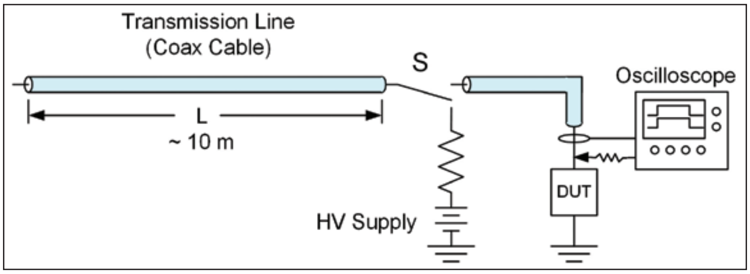

Figure 2: (Over) simplified TLP system for a 100 ns pulse

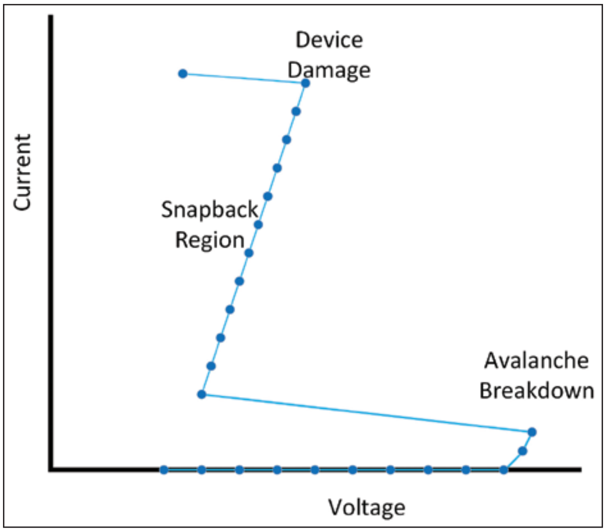

Figure 3: Sample IV curve from a TLP measurement

reflections. Several methods have been developed to remove reflections and some of them will be discussed in these two articles.

Other factors result in a proliferation of TLP types. TLP systems are high speed systems requiring signal paths that maintain a constant impedance except for the DUT itself. The challenges of high-speed measurements are especially true for pulse lengths below 10 ns, to the extent that such systems get their own name, very fast TLP (vf-TLP). The characteristic impedance of the TLP system can also affect the resultant measurement, potentially hiding important characteristics of the DUT. To explore the challenges and solutions in TLP measurements, several TLP variations will be discussed, time domain reflection in this article and several other configurations in Part 2.

TIME DOMAIN REFLECTION TLP

The most common form of TLP is the Time Domain Reflection (TDR) system shown in Figure 4. This is essentially the same as that shown in Figure 2 except for the insertion of the attenuator, which is frequently about 6 dB, reducing the signal by half. This is a good time to describe what happens during a single TLP pulse.

The transmission line is first charged to a voltage. The relay S is then closed, initiating the pulse. The pulse travels through the attenuator and is measured by the oscilloscope using current and voltage probes. The pulse continues to the DUT where some of the current passes through the DUT and the remainder of the pulse is reflected back towards the pulse source. The reflected pulse is then measured again by the voltage and current probes. The pulse then travels back through the attenuator, travels the full length of the transmission line, is reflected back toward the DUT passing through the attenuator for a third time. The second and third passes of the pulse through the attenuator ensure that after the initial stress on the DUT each subsequent stress is reduced by at least a factor of four.

In TLP systems the voltage and current probes are often placed some distance from the DUT. This is done because it is often easier to maintain a constant impedance at the position of the probes at a position away from the DUT. This is especially true when doing wafer probing. To determine the voltage and current at the DUT, it is necessary to rely on the reflection properties of signals traveling in coaxial cables when they meet a change in impedance. These properties are described by the following equations, where VI and II are the incident voltage and current, VR and IR are the reflected voltage and current, and ZCable and ZDUT are the cable and DUT impedances.

$$V_R = V_I \frac{Z_{DUT} - Z_{Cable}}{Z_{DUT} + Z_{Cable}} \qquad I_R = -I_I \frac{Z_{DUT} - Z_{Cable}}{Z_{DUT} + Z_{Cable}}$$

The voltage and current which the DUT experiences is the sum of the incident and reflected signals. The TDR method can be used for standard, 100 ns pulse length, TLP, and for vf-TLP with pulse lengths in the 5 ns or shorter range. How the signals are handled is different for 100 ns TDR and for 5 ns TDR, as shown in Figure 5.

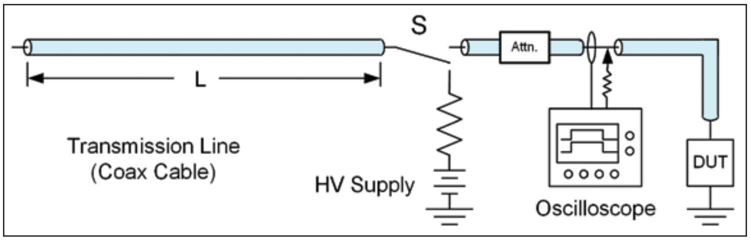

Figure 4: Time Domain Reflection (TDR) TLP system for standard or vf-TLP

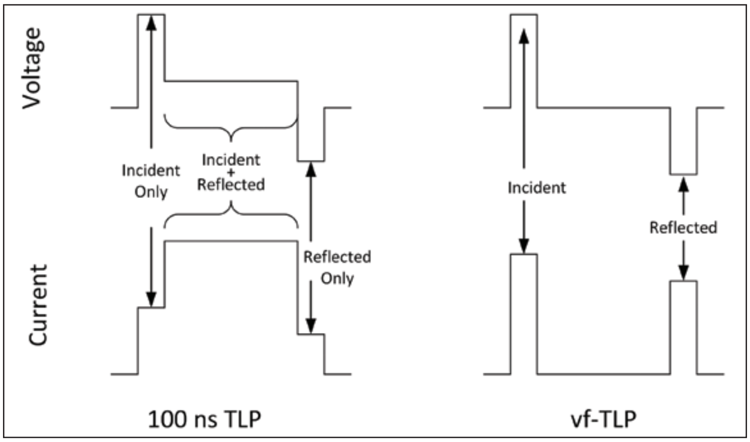

Figure 5: TDR oscilloscope traces for standard and vf-TLP for a DUT with impedance less than 50 ohms

For a 100 ns TLP pulse the pulse length is long enough that the incident and reflected pulses overlap at the position of the probes. Since the incident and reflected pulses overlap at the probe positions, the voltage and current can be directly measured during the overlap period. Typically, the voltage and current are averaged over a time window late in the overlap period. This method creates high quality I-V curves of the type discussed in Figure 3.

This cannot be done with vf-TLP because the pulse length is too short for there to be sufficient, or any, overlap at the probes of the incident and reflected signals. For vf-TLP it is necessary to have the probes and DUT sufficiently separated that the pulses have no overlap. The digital data from the oscilloscope is used to time shift the incident and reflected pulses numerically and then add them together to obtain the voltage and current experienced by the DUT. An advantage of the vf-TLP method is that the time dependence of the voltage and current can be observed directly in the added signals. The disadvantage is that vf-TLP I-V curves are often much noisier than for 100 ns TLP. This is because for a low resistance DUT the vf-TLP voltage measurement is the subtraction of two large numbers while the 100 ns TLP is a direct measurement. In vf-TLP care must also be taken to obtain the proper amount of time shift when adding the incident and reflected signals or critical time dependent features can be distorted.

The above discussion for TDR TLP implies that the 100 ns TLP and vf-TLP measurement systems are the same except for the length of the charged cable which determines pulse length. This is true in principle but usually not in practice. Measuring I-V curves with 100 ns TLP is relatively forgiving of less-than-ideal test fixturing. Short clip leads and standard wafer probes can be used to connect from the coax pulse source to the DUT. The voltage probe can be a standard 500 MHz oscilloscope probe and the current probe can be a Tektronix CT1 probe in an appropriate fixture. This is not the case for vf-TLP, where maintaining 50-ohm impedance right up to the DUT is critical. For wafer level measurements, RF probes become a requirement. To obtain the required bandwidth for voltage measurements, voltage pickoff Tees with resistances between 1000 and 5000 ohms are used rather than oscilloscope voltage probes. For vf-TLP current measurements are often obtained from the voltage data using I = V/50 ohms due to bandwidth limitations of current probes. In 100 ns TLP with overlapping incident and reflected pulse, device current cannot be determined from the voltage measurement because the voltage does not contain the needed directional information for a current measurement. In vf-TLP with separated incident and reflected currents, the directional information is known.

SUMMARY

In this article, some of the fundamental aspects of TLP testing have been introduced along with the most widely used TLP configuration, time domain reflection. The second article, to be published next month, will introduce more members of the TLP Zoo, Kelvin TLP, time domain reflection and transmission TLP, and current source TLP. The importance of a TLP system's characteristic impedance will also be covered. Finally, two extensions of the TLP Zoo that promise improved CDM testing at low voltages where the traditional field induced CDM test methods have limitations will be discussed. A section on additional TLP reference documents will be included.

REFERENCES

1. "For Electrostatic Discharge Sensitivity Testing Human Body Model (HBM) – Component Level," ANSI/ESDA/JEDEC JS-001.
2. "For Electrostatic Discharge Sensitivity Testing Charged Device Model (CDM) – Component Level," ANSI/ESDA/JEDEC JS-002.
3. "Electromagnetic compatibility (EMC) - Part 4-2: Testing and measurement techniques - Electrostatic discharge immunity test," IEC 61000-4-2.
4. N. Khurana, T. Maloney, and W. Yeh, "ESD on CHMOS Devices - Equivalent Circuits, Physical Models and Failure Mechanisms," Proceedings of 23rd International Reliability Physics Symposium, 1985.
5. T. Maloney and N. Khurana, "Transmission Line Pulse Techniques for Circuit Modeling of ESD Phenomena," Proceedings of the EOS/ESD Symposium, 1985.

Advertiser Index

Upcoming Events

February 7

ESD Best Practices for Technology Change

February 8-10

Applying Practical EMI Design and Troubleshooting Techniques

Advanced PCB Design for EMC & SI

February 13-18

European Microwave Week

March 8-11

EMC Compo

March 15-17

EMV 2022

March 27-April 1

EuCAP 2022 – The 16th European Conference on Antennas and Propagation

April 3-6

A2LA Tech Forum 2022

April 5-7

DesignCon 2022

April 19

EMC mini 2022

April 18-22

EMC Week

April 28-29

Principles of Electromagnetic Compatibility

Due to COVID-19 concerns, events may be postponed. Please check the event website for current information.